

ADDIS ABABA UNIVERSITY
ADDIS ABABA INSTITUTE OF TECHNOLOGY
AFRICAN RAILWAY CENTER OF EXCELLENCE



Effect Of Ballast On The Dynamic Behavior Of RC T-Girder Railway Bridge

A Thesis in Railway Engineering(Civil Infrastructure)

By Abdelmalik Mohammed

February 25, 2020

Addis Ababa

A Thesis

Submitted in Partial Fulfillment of the Requirements for the Degree of Master of Science

The undersigned have examined the thesis entitled '**Effect Of Ballast On The Dynamic Behavior Of RC T-Girder Railway Bridge**' presented by **Abdelmalik Mohammed**, a candidate for the degree of **Master of Science** and hereby certify that it is worthy of acceptance.

Dr. Abraham Gebre

Advisor

Signature

Date

Mr. Ntakyemungu Mathieu

Internal Examiner

Signature

Date

Dr. Asnake

External Examiner

Signature

Date

Chair person

Signature

Date

UNDERTAKING

I certify that research work titled “**Effect of Ballast on the Dynamic Behavior of RC T-Girder Railway Bridge**” is my own work. The work has not been presented elsewhere for assessment. Where material has been used from other sources it has been properly acknowledged / referred.

Abdelmalik Mohammed

Acknowledgements

I have experienced help from many persons in conducting research under hectic conditions and writing a thesis. It is quite impossible to list all the contributors by name. However, I would still like to take an opportunity and privilege to acknowledge a few who have helped me in the consistent learning process I have passed through.

First and foremost, I am grateful to the Allah for the good health and well-being that is necessary to complete my study. I would like to express my sincere gratitude to my advisor Dr. Abrham Gebre , for the continuous support of my MSc thesis, for his patience, motivation and immense knowledge. His guidance helped me in all the time of research and writing of this thesis.

There are no words to express my appreciation to Woldia/Haragebeya –Mekelle Railway project Engineers in the study site. Words may not sufficient to acknowledge their contributions. I am grateful to my best friend Mr. Hailemariam Assefa, who helped me in ups and downs in gathering data and field work.

Last but not list, I would like to thank my family and friends for supporting me spiritually throughout writing thesis and my life in general.

Abbreviations/Symbols

3D = Three Dimension

AS= Australian Code

C= Rayleigh damping coefficients

CWR = Continuous Welded Rail

ERRI = European Rail Research Institute

FEM = Finite Element Method

HRB = Hot Rolled Ribbed Bar

HPB =Hot Rolled Plain Bar

LAA = Los Abrasion Test

K= Stiffness

M= Mass

RC= Reinforced Concrete

TB/T = Chinese Standard

TS = Railway Quality Management System

UIC = Union International Des Chemn Defr

ω = Radial vibration Frequency (rad/sec)

ω_e = Eigen Frequency (rad/sec)

$H_{\omega F}$ = Complex transfer function from force to displacement (m/N)

$S_{\omega \omega}$ = Autospectrum of Displacement (m²s)

S_{FF} = Autospectrum of the force (N²s)

f = Vibration frequency (Hz)

Contents

Acknowledgements.....	1
Abbreviations/Symbols.....	2
Abstract.....	7
1. Introduction.....	8
1.2. Statement Of The Problem	9
1.3. Objectives Of The Study.....	9
1.3.1. Main Research Objective	9
1.3.2. Specific Research Objectives.....	10
1.3.3. Research Questions.....	10
2 Literature Review.....	11
2.1Components Of Rail Track	11
2.1.1Rails	12
2.1.2 Fastening System	12
2.1.3Sleeper.....	12
2.1.4Ballast	13
2.1.5 Subballast.....	15
2.2 Prestressed T-Beam.....	16
2.3 Vertical dynamic behavior	18
2.3.1 Dynamic Properties of the Track	18
2.4 Track modelling techniques	20
2.5 Modeling of Ballast and Its Dynamic effect On Bridge.....	21
3. Methodology	24
3.1static Load Test.....	24
3.2 Finite Element Analysis	24
3.3 Analysis Type	24
3.3.1 Computational model.....	25
3.3.2 Model verification.....	25
3.3.3 Transient analysis.....	25

3.3.4 Sensitivity analysis.....	25
4. Numerical Modeling of Ballasted RC T-Girder Bridge.....	26
4.1 FEM Model for the Ballasted Rc T-Girder Bridge Using Abacus.....	26
4.1.1 Material properties.....	26
4.1.2 Modelling of Bridge component.....	27
4.1.2.1 FEA Element Types used in the model.....	27
4.2 Validation and Eigen value analysis of the FEM model.....	32
4.2.1 Validation of the FEM model (Static load simulation).....	32
4.2.2 Testing Of The Bridge.....	33
4.2.3 Geometry of the prestressed T-girder railway bridge.....	34
4.2.4 Production and Erection.....	36
4.2.5 Experimental Model Loading.....	38
4.3 FEM Modeling of Static Load Test.....	40
4.4 Analysis of Effect of ballast on the dynamic behavior of RC T-girder.....	43
4.4.1 ABAQUS Model Modal Analysis.....	43
Case-1 (Prestressed T-Girder Bridge Model Alone(T)).....	44
Case-2 (Prestressed T-Girder and ballast Model Alone(TB)).....	45
Case-3 (Prestressed T-Girder, Ballast and Sleeper Model Alone(TBS)).....	47
Case-4 (The Whole Bridge With Spring Rail To Sleeper Model (TBSR)).....	48
4.5 Finding.....	50
5 Sensitivity Analysis.....	52
5.2.1 Effect of stiffness of ballast.....	52
5.2.2 Effect of ballast density.....	53
5.2.3 Effect of ballast depth.....	54
5.2.4 Effect of support condition.....	55
6. Conclusion and Recommendation.....	57
6.1 Conclusion.....	57
6.2 Recommendation.....	57
7. References.....	59
8. Annex.....	60
8.1 static load test result on the T-girder.....	60

8.2 Mode Shape Frequency values of Each FEM model	62
---	----

Table of Figures

Figure 2-1: component of railway track.....	11
Figure 2-2: Cross section of railway track	11
Figure 2-3 : Response of prestressing- and reinforcement steel (after Sacdirat. K et al 2007)	16
Figure 2-4: Load-displacement of prestressed- and reinforced concrete members subjected to an axial tensile force (after Sacdirat. K et al 2007).....	17
Figure 2-5: Load-displacement curve for an eccentric prestressed beam (after Sacdirat. K et al 2007)	17
Figure 2-6: Track receptance at the exciting point. Mid-span excitation (-). Excitation above a sleeper (- -). The mode shapes are qualitatively represented.....	19
Figure 2-7. simplified models of ballasted track: considering the ballast without a vibrating mass (a) and considering the ballast as a vibrating mass (b).	21
Figure 2-8: Model of the ballast under one rail support point.....	22
Figure 4-1: modeling of beam element	28
Figure 4-2: UIC 54 rail cross section (After UIC standard).....	29
Figure 4-3: 3D Solid model of ballast.....	30
Figure 4-4:)a) 3D solid, b)Reinforcement detail, c)Cross section and d)meshed model of prestressed T- girder	31
Figure 4-5: Location of the T-girder bridge	33
Figure 4-6: Longitudinal section of the T- girder.....	35
Figure 4-7: Cross-section of the T- girder.....	35
Figure 4-8: Reinforcement detail for prestressed T- girder bridge.....	36
Figure 4-9: Production stage of the bridge	37
Figure 4-10: Erection of the bridge (On-site placement)	37
Figure 4-11: Load application on Prestressed T-girder bridge.....	38
Figure 4-12: static load test (On-site experiment).....	39
Figure 4-13: modeling of static load test by ABAQUS and its result	41
Figure 4-14: Deflection versus load graph for the experiment and model.....	42
Figure 4-15: The undeformed shape and meshed model.....	44
Figure 4-16: Undeformed shape of ballast and T-girder model	45
Figure 4-17 a: The first eight mode shapes of the model	46
Figure 4-18: Undeformed shape and meshed sleeper,ballast and T-girder model	47
Figure 4-19 : Longitudinal resistance of Vossloh W14 Clamp Slk 14 fastner node	48
Figure 4-20: Undeformed shape and meshed Rail, sleeper, ballast and T-girder model.....	49
Figure 4-21: Frequency vs Mode graph for each model	51
Figure 5-1: Frequency vs Mode graph for various ballast stiffness	53
Figure 5-2: Frequency vs Mode graph for various ballast density	54
Figure 5-3: Frequency vs Mode graph for various ballast depth.....	55
Figure 5-4: Frequency vs Mode graph for different bridge support condition.....	56

Figure 8-1: The first eight mode shapes of the model (Case1)	62
Figure 8-2: The first ten natural frequencies of the model (Case1).....	63
Figure 8-3: The first four mode shapes of the model (Case3).....	63
Figure 8-4: The 5 th to 10 th mode shapes of the model (Case3).....	64
Figure 8-5: The first ten natural frequencies of model (Case3)	65
Figure 8-6: The first four mode shapes of the model (Case4).....	65
Figure 8-7: The 5 th to 10 th mode shapes of the model (Case4).....	66
Figure 8-8: The first natural frequencies of the model (Case4)	67

List of Tables

Table 2-1: size and gradation of ballast as specified by both AS 2758.7 (1996) and TS 3402 (2001)	14
Table 2-2: Minimum ballast strength and maximum strength variation (AS 2758.7).....	14
Table 2-3: Ballast Specifications in Australia, USA and Canada (after Indraratna et al.,2002c).....	15
Table 4-1: Material property of track component and T- girder (After Material Specification of T-girder in Woldia/Haragebeya-mekelle Railway Bridge, 2014)	27
Table 4-2: static load test result on the T-girder.....	40
Table 4-3 : load deflection relation of static load model at mid span	42
Table 4-4 : Brief description of the models' parameter	44
Table 4-5: The first ten modes frequencies	45
Table 4-6: The first ten modes frequencies	47
Table 4-7: The first ten modes frequencies	48
Table 4-8: The first ten modes frequencies	49
Table 4-9: Summary of frequencies and modes of vibration from the numerical models	51
Table 5-1 Parameters to be studied on sensitivity analysis	52
Table 5-2: Influence of ballast elastic modulus on vibration frequencies	52
Table 5-3 : Influence of ballast ballast density on vibration frequencies	53
Table 5-4: Influence of ballast depth on vibration frequencies	54
Table 5-5: Influence of support condition of bridge on vibration frequency	55
Table 5-6: Frequency vs Mode graph for different bridge support condition	56

Abstract

Due to modernization of the railway transportation sector, as high speed railway lines have become more common, nowadays researches are being carried to assess and analyse the properties of the track and its component besides its effect on the overall bridge dynamics.

Dynamic responses of the railway track and its elements are key parameters to measure the structural capability of railway track and its elements. If a dynamic loading resonates the railway track's dynamic responses, its elements tend to possess damage from excessive dynamic stresses. For instance, a rail vibration leads to defects in rails or wheels. The track vibrations will cause the crack harm in railway sleepers or fasteners, or maybe the breakage of ballast support. Therefore, the identification of dynamic properties of ballasted railway track and its elements is very essential, so as to avoid any train operation which may trigger such resonances.

In this thesis, 3D FEM models that represent the ballast as a solid part were modelled. Such systems of modeling take sensible advantage of the capability of contemporary FEM package (Abaqus) in modeling the continuity of the track beyond the bridge by imposing applicable boundary conditions on the railway line. And a static load test was conducted on one tracked Prestressed T-girder railway bridge to check its stiffness. Data from the tests was processed, and modeling the prestressed tendon like embedded element give more realistic result compared to assuming it like cohesive element with concrete girder.

The objective of this thesis is to investigate the effect of ballast the dynamic behavior of T-girder Railway Bridge. Hence its effect on the dynamic properties of the bridge was assessed in this thesis by implementing and comparing different 3D FEM models of the bridge that describe different structure and track configurations. Model that included the ballast alone showed a drop by (2.09-17.63)% in the natural frequency for vibration mode 1-4th and 10th and a rise by (3.07-16.52)% in the natural frequency for 5-9th mode of vibration were observed as compared to the model that accounted for the mass of the T-girder bridge only. In addition, different parameters influencing the natural frequencies and modes shapes of the bridge were tested and it appears that the ballast introduces considerable additional stiffness for 5-9th mode of vibration. Density, stiffness, depth of ballast and support condition parameters as well was found to affect the dynamic properties of the bridge.

Keywords: Prestressed T-girder Railway bridges, Ballast, static load test, Finite element modelling, Bridge dynamics, Modal analysis(Eigen mode analysis)

1. Introduction

Railway track performance is influenced by its parts so it's attainable to realize higher performance by understanding constituent parameters of tracks and modifying them. The most vital parameter about the dynamic analysis of a railway track is estimation of natural frequency. Natural frequency is that the frequency at that a structure vibrates once excited by a transient load or once left undisturbed.

Structural dynamic issues could lead in a significant failure and design restriction over a wide range of engineering structures since natural phenomena and human activities typically impart time-dependent burden on each accessible structures. Hence Analysis and design of these structures take into consideration dynamic action.

The dynamic parameters of these structures, like natural frequency, damping constant, and corresponding vibration mode have considerable importance within the procedures required for analysis and design of such structures subjected to dynamic loadings. Consequently, it's very essential to study the dynamic and acoustic properties of an structure that are subjected to numerous sources of noise and vibration. In general, the foremost outcomes of the vibration measurements are the natural frequency, the dashpot worth and the mode shape.

The stiffness can be extracted and calculated from the static load responses of structures. The principal reason of the static load test is that that result can allow verification of the analytical model proposed for the system tested. The analytical model, which has been verified, may be employed in design and response prediction with much confidence. It forms a new arena in engineering trials as an experiment. However, the structural modifications in computer simulations could yield further sensitivity analysis whereas either linear or nonlinear behavior can be identified through the experimentations.

Enormously, railways have been playing major role in transporting population, resources, merchandises, etc. over the big continent of any country. Railway business has shown considerable growth within the past century and has continually developed new appropriate technology for its solution to specific necessities. In several countries, the normal line is that the ballasted track, that consists of rails, rail pads, and concrete sleepers laid on ballast and subgrade.

Recently, the demand of track usages has greatly inflated. The rise in frequency of traffic for passenger trains and the increase in loads of various freight trains over recent years have also been a big issue tributary to the deterioration of the railway track system. The rise in transport capability has been aroused by the growing industrial demand for long-distance freight conveying, particularly in giant countries with several coalmines like Australia or China. It absolutely was evident that railway tracks in Australia are deteriorating because of inflated traffic frequency, heavier wheel hundreds and improper maintenance.

Regardless to a nature that railway tracks are subject to impact dynamics originated by wheel/rail interaction or irregularities, railway civil engineers have paid attention to the capability of track elements under realistic load. This has been a recent plan to develop the advances in style of such infrastructure

From railway component this thesis will investigate how ballast material affects the dynamic property of prestressed T-girder Bridge by taking into consideration different ballast properties such as density, stiffness, depth and finally the influence of support condition of the bridge itself.

Although studies show that the track has a significant influence on the bridges vibrations and, possibly on the stiffness of the whole bridge itself, the contribution of the ballast to the bridge stiffness is still in study. Indeed, the natural frequency of structure is proportional to the square root of the stiffness divided by the mass. The mass and stiffness are two antagonist parameters in relation to the natural frequency and it's crucial to know and understand how the ballast affects this two parameters.

1.2. Statement Of The Problem

Ethiopian Railway Corporation has identified eight railway corridors for study, design and subsequent implementation, the total length of which is around 5060km. Addis Ababa-Dewale and Woldia/Haragebeya –Mekelle route used Chinese class II standard railway line and implemented prestressed RC T- Girder Bridge For lower spans up to 35m. T-beam girder is adopted for economical reason moreover it is easy to install and maintain.

The corporation has a plan to design and implement the other six corridors in the future. Hence to deal with a rapid development of speed of trains and railway technology, constant improvement of the railway infrastructure is necessary and engineers are continuously facing challenges in order to design efficient and optimized structures. Due to this fact a comprehensive understanding of the dynamic behaviour of structures leads to an efficient and sound design that meets imposed safety and comfort requirements.

The railway transportation sector today, where high speed railway lines are becoming more and more common, demands for knowledge of the behaviour of railway bridges is very essential. A railway bridge is composed of the main load bearing structure and track, which includes the ballast, sleepers and the rails, and the non-structural elements. The dynamic behaviour of the load bearing structure, which is usually made of concrete or steel or their combination, has been investigated for long and is known to a sufficient level of details. However, the amount of effect of the track/ballast on the dynamic behaviour of railway bridges is still a research question. This thesis will present a study to be performed with the purpose of providing the effects of the ballast of railway track on the dynamic behaviour of a prestressed RC T- girder bridge. Moreover It addresses the different methods to model the various types of track, as well as the influence of different parameters (stiffness, density, and thickness) of ballast in the natural frequencies and modes shapes of the bridge will be tested.

1.3. Objectives Of The Study

1.3.1. Main Research Objective

This master thesis aims at quantifying the influence of the ballast on the dynamic properties of a bridge. It shows if the ballast gives just additional mass on the structure or if it introduces any additional stiffness. The thesis also aims at assessing the influence of the ballast and track components on the dynamic properties of the

bridge by examining the degree of influence of the mentioned components in providing additional stiffness to the bridge.

1.3.2. Specific Research Objectives

- 1) Analyse the results of the static load test on the T- girder bridge that to be used on Woldia/Haragebeya- Mekelle railway project.
- 2) Prepare the numerical model, including the track and the ballast, to achieve the good representation with the real situation.
- 3) The thesis investigates the effect of the ballast on the natural frequencies and it aims also at determine if the ballast contributes any additional stiffness to the T-girder bridge.
- 4) Analyse the effect of parameter(density, stiffness and support condition)s that characterize ballast on natural frequency of T- Girder Bridge.

1.3.3. Research Questions

The main research question is:

“Is the ballast just an additional mass on the structure or does it introduce any additional stiffness?”

In order to answer this general question, the following specific questions have been developed:

1. How to analyze the results of the static load test on the T- girder bridge.
2. How to create the numerical model, including the track and the ballast, to achieve the good correlation with the real situation.
3. How the natural frequencies of the bridge corresponding to several eigenmode can be extracted?
4. How to analyze the impact of the ballast and track component on the dynamic behaviour of T- Girder Bridge?
5. How parameters that characterize ballast affect the natural frequencies of the T- girder bridge and gives any additional stiffness to the bridge.

2 Literature Review

2.1 Components Of Rail Track

A ballasted track system consists of the following components: (a) rail, (b) fastening system, (c) sleepers or ties, (d) ballast, (e) subballast and, (f) subgrade. The subballast and subgrade are replaced by bridge in presence of bridge structures or any super structures. Figure 2.1&2.2 show a typical track section and its different components. The track components may be grouped into two main categories: (a) superstructure, and (b) substructure.

Track superstructure consists of rails, fastening system and sleepers. The substructure comprises ballast, subballast and subgrade. The superstructure is separated from the substructure by the sleeper-ballast interface.

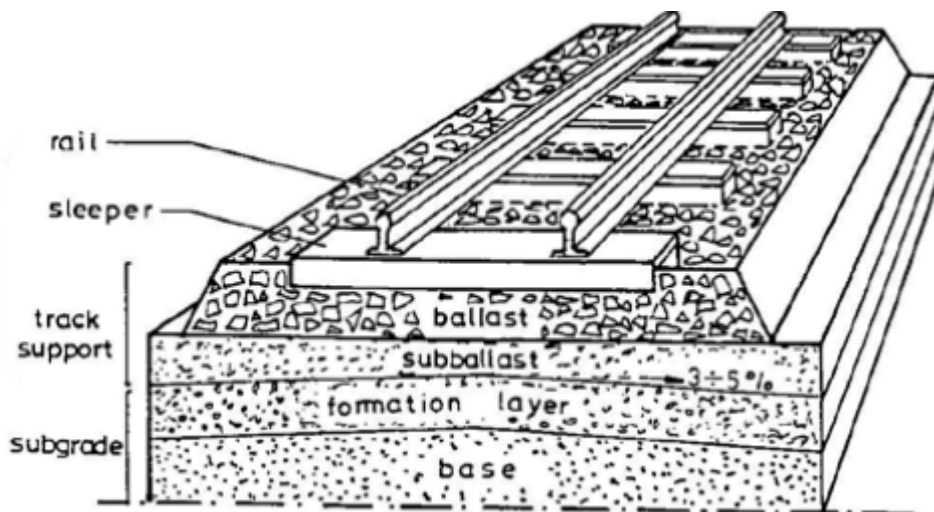


Figure 2-1: component of railway track

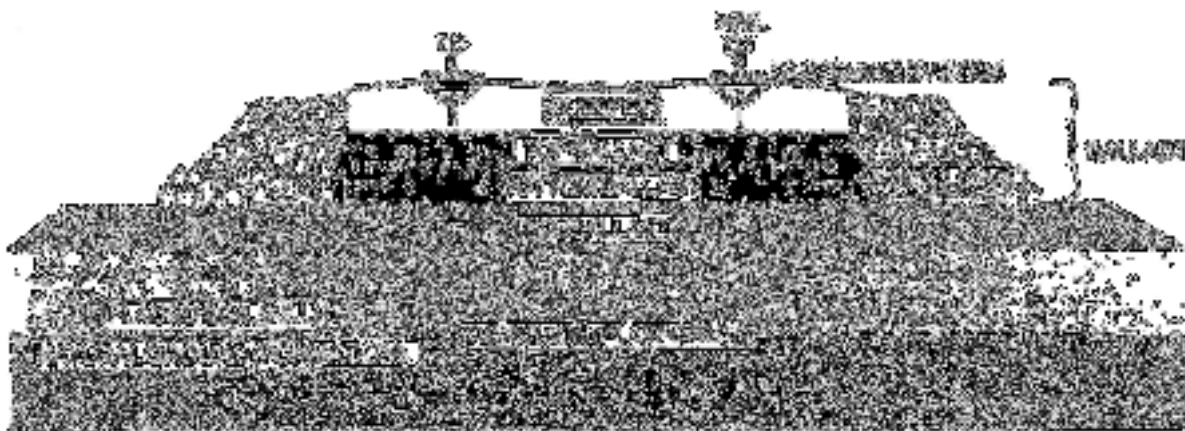


Figure 2-2: Cross section of railway track

2.1.1 Rails

Rails are longitudinal steel members that guide and support the train wheels, and transfer concentrated wheel loads to the supporting sleepers, which are spaced evenly along its length. The rails must be stiff enough to carry out the above functions without excessive deflection between the sleepers. The rails may also serve as electric signal

conductors and as the ground line for electric power trains. The vertical and lateral profiles of the rails and the wheel profile govern the smoothness of traffic movement as the wheels roll over the track. Consequently, any appreciable defect on the rail or wheel surface can cause a significant magnitude of dynamic load on the track structure when the trains are running fast. Excessive dynamic loads caused by rail or wheel surface imperfections are detrimental to other components of the track structure.

Rail sections may be connected by bolted joints or welding. In bolted joints, the rails are connected with drilled plates known as 'fishplates'. However, the discontinuity resulting from this joint causes vibration and extra dynamic load, which lowers passenger comfort and causes accelerated failure around the joint. The combination of impact load and reduced rail stiffness at the joints produces exceptionally high stress on ballast and subgrade, and this increases the rate of ballast degradation, fouling, and settlement. Most track problems are found at bolted rail joints where frequent maintenance is required. Therefore, nowadays most of passenger and heavily used freight lines, bolted joints have now been changed by continuously welded rail (CWR). CWR has several importances, including savings in maintenance due to the minimization of joint wear and batter, improved riding quality, reduced wear and tear on rolling stock, and reduction in substructure damage (Selig and Waters, 1994).

2.1.2 Fastening System

Steel fasteners are used to hold the rails on the sleepers to ensure they do not move vertically, longitudinally, or laterally (Selig and Waters, 1994). Various types of fastening systems are used by railway organisations throughout the world, depending on the type of sleeper and geometry of the rail section.

The major components of a fastening system include coach screws to hold the baseplate to the sleeper, clip bolts, rigid sleeper clips, spring washers and nuts to attach the sleeper to the rail (Esveld, 2001). Rail pads are sometimes used on top of the sleepers to dampen the dynamic forces generated by high-speed traffic movements. Fasteningsystems are categorised into two groups: direct fastening and indirect fastening. In direct fastening, the rail and baseplate are connected to the sleeper using the same fastener. In contrast, in an indirect fastening system, the rail is connected to the baseplate with one fastener, while the baseplate is attached to the sleeper by a different fastener (Esveld, 2001). The indirect fastening system allows a rail to be removed from the track without removing the baseplate from the sleeper, and allows the baseplate to be attached to the sleeper before being placed on the track.

2.1.3 Sleeper

Sleepers (or ties) provide a solid, even and flat platform for the rails, and form the basis of a rail fastening system. They hold the rails in position and maintain the designed rail gauge. Sleepers are laid on top of compacted ballast layer, perpendicular to the rails, and at a specific distance apart. Mechanically, sleepers are

subjected to concentrated lateral, vertical and longitudinal forces from the wheels and rails, and transfer them over a wider ballast area to minimize the stress to an acceptable level. Sleepers can be made of wood, concrete or steel. However, timber sleepers are predominantly used worldwide. In recent times, prestressed concrete sleepers have become popular and economic in several countries. Steel sleepers are expensive and are used only in special situations. Timber sleepers are cheaper and available in most parts of the world. Prestressed concrete sleepers are potentially more durable, stronger, heavier, and more rigid than timber sleepers. Moreover, the geometry of the concrete sleepers can be easily modified to extend the support area beneath the rails. The extended support area decreases ballast/sleeper contact stress, which minimizes track settlement and particle breakage. Concrete sleepers provide an overall stiffer track, which also increases fuel consumption benefits. Some researchers however, indicate that timber sleepers are more resilient and less abraded by the surrounding ballast compared to concrete sleepers (Key, 1998).

2.1.4 Ballast

The term 'ballast' used in railway engineering means granular coarse aggregates placed above subballast or subgrade to act as a firm platform with high bearing capacity, and support the track superstructure (sleepers, rails etc.). The sleepers (or ties) are embedded into the ballast layer. Ballast is usually composed of crushed rocks originating from high quality igneous or well-cemented sedimentary rock. Traditionally, crushed angular hard stones and rocks having uniform gradation, free of dust, and not prone to cementing action have been considered good quality ballast materials (Selig and Waters, 1994).

The source of ballast (parent rock) varies from country to country depending on the quality and availability of the rock, and economy. No standard specification of ballast for its index characteristics such as size, shape, hardness, abrasion resistance and mineral composition that will provide the best track performance under all types of loadings, subsoil and environments, has yet been established. Because there are no such standard specifications, a wide variety of materials (e.g. basalt, limestone, granite, dolomite, rheolite, gneiss, slag, gravel etc.) are used as ballast throughout the world.

2.1.4.1 Functions of ballast

Ideally, ballast should perform the following functions (Jeffs, 1989):

- ✓ Provide a firm and stable platform, and support the sleeper uniformly with high bearing capacity
- ✓ Transmit the high imposed pressure at the sleeper/ballast interface to the subgrade layer at a reduced and acceptable stress level
- ✓ Provide adequate stability to the sleepers against vertical, longitudinal and lateral forces generated by train movements within designed speed limits
- ✓ Provide dynamic resiliency
- ✓ Provide adequate resistance against crushing, attrition, bio-chemical and mechanical degradation and weathering
- ✓ Provide minimal plastic deformation to the track structure
- ✓ Provide adequate hydraulic conductivity for drainage purposes
- ✓ Facilitate maintenance operations
- ✓ Inhibit weed growth

- ✓ Absorb noise, and
- ✓ Provide adequate electrical resistance.

2.1.4.2 Properties of ballast

In order to fulfil the above functions satisfactorily, ballast must have certain characteristics such as particle size, shape, gradation, surface roughness, particle density, bulk density, strength, durability, hardness, toughness, resistance to attrition and weathering, as discussed below. Various standards and specifications are made by railway organisations throughout the world to meet their ballast requirements. In general, ballast particles must be angular, uniformly graded, strong, tough and durable under anticipated traffic loads and environmental changes. In Australia, Australian Standard AS 2758.7 (1996) specifies the general requirements, and the specification TS 3402 (2001) details the specifications and required properties of ballast for Rail Infrastructure Corporation (RIC) of NSW. The size and gradation of ballast as specified by both AS 2758.7 (1996) and TS 3402 (2001) are given in table 2.1.

Sieve size (mm)	% passing by weight
	(Nominal ballast size = 60 mm)
63.0	100
53.0	85-100
37.5	20-65
26.5	0-20
19.0	0-5
13.2	0-2
9.50	-
4.75	0-1
1.18	-
0.075	0-1

Table 2-1: size and gradation of ballast as specified by both AS 2758.7 (1996) and TS 3402 (2001)

The Australian Standard AS 2758.7 (1996) also specifies the minimum wet strength and the wet/dry strength variation of the ballast particles when determined in accordance with AS 1141.22 for the fraction of aggregates passing 26.5 mm sieve and retained on 19.0 mm sieve, as shown in table 2.2.

Minimum wet strength (kN)	Wet/dry strength variation (%)
175	≤ 25

Table 2-2: Minimum ballast strength and maximum strength variation (AS 2758.7)

The durability of ballast is usually assessed by conducting several standard tests such as Los Angeles Abrasion (LAA) test (AS 1141.23), Aggregate Crushing test (AS 1141.21), Wet Attrition test (AS 1141.27) etc. Indraratna et al. (2002c) gives a comparison between the specifications of ballast used in Australia (AS 2758.7), USA (Gaskin and Raymond, 1976) and Canada (Gaskin and Raymond, 1976; Raymond, 1985), as given in Table 2.3.

Ballast property	Australia	USA	Canada
Aggregate Crushing Value	< 25%		
LAA	< 25%	< 40%	< 20%
Flakiness Index	< 30%		
Misshapen Particles	< 30%		< 25%
Sodium Sulphate Soundness		< 10%	< 5%
Magnesium Sulphate Soundness			< 10%
Soft and Friable Pieces		< 5%	< 5%
Fines (< No. 200 sieve)		< 1%	< 1%
Clay Lumps		< 0.5%	< 0.5%
Bulk Unit Weight	> 1200 kg/m ³	> 1120 kg/m ³	
Particle Specific Gravity	> 2.5		> 2.6

Table 2-3: Ballast Specifications in Australia, USA and Canada (after Indraratna et al.,2002c)

In order to design the track substructure adequately and efficiently, it is essential to know the magnitude of sleeper/ballast contact stress and the distribution of stresses through the ballast, sub-ballast and subgrade layers. The depth of ballast layer required for a track structure depends on the maximum stress intensity at the sleeper/ballast interface, acceptable bearing pressure of the underlying layer (subballast or subgrade) and the distribution of vertical stress through the ballast layer. Several methods, including simplified theoretical models, semi-empirical and empirical solutions are used in practice to determine the distribution of vertical stress through the ballast layer (Doyle, 1980). These methods are based on estimating stress under a uniformly loaded strip of infinite length and circular loaded area.

2.1.5 Subballast

Subballast is a layer of aggregates placed between ballast layer and the subgrade, and usually comprised of well-graded crushed rock or sand/gravel mixtures. It prevents entrance of coarse ballast grains into the subgrade, and also prohibits upward migration of subgrade particles (fines) into the ballast layer. Subballast therefore, acts as a filter and separating layer in the track substructure, transmits and distributes stress from the ballast layer down to the subgrade over a wider area, and also acts as a drainage medium, to a limited extent. When designing the subballast layer, attention must be given to its filtering function. Therefore, it is mostly made of widely graded materials where the empirical filter design methods govern its particle size distribution. Where there is no subballast or where poorly designed subballast is used, subgrade clay and silt size particles

become mixed with ground/infiltrated water to form a slurry, which is pumped up to the ballast layer under cyclic loading (clay pumping). In low lying coastal areas of Australia and many other parts of the world, ballast fouling by clay pumping is commonly observed during and after heavy rainfall.

2.2 Prestressed T-Beam

Pre-stressing is introduced into a structure so that the designer can get an even better crack control. This is beneficial when there is a need to maintain the rigidity of the uncracked structure, when there is a risk of corrosion of reinforcement due to open cracks, to prevent fatigue of the reinforcement or when there are high demands on the tightness of the structure. It is important to point out that the prestressing does not noticeably influence the flexural resistance of the member, but mainly delays the upcoming of cracks (Engström, 2011).

The principal stress-strain relationship as well as an idealized stress-strain relationship for prestressing steel (cold worked steel) can be seen in Figure 2.3a. It should be noted that the strength of the prestressing steel is larger than the strength of ordinary reinforcement steel, but at the same time it lacks the ability to deform very much before failure. To clarify these property differences the working curve of regular reinforcement is also included in the figure 2.3b.

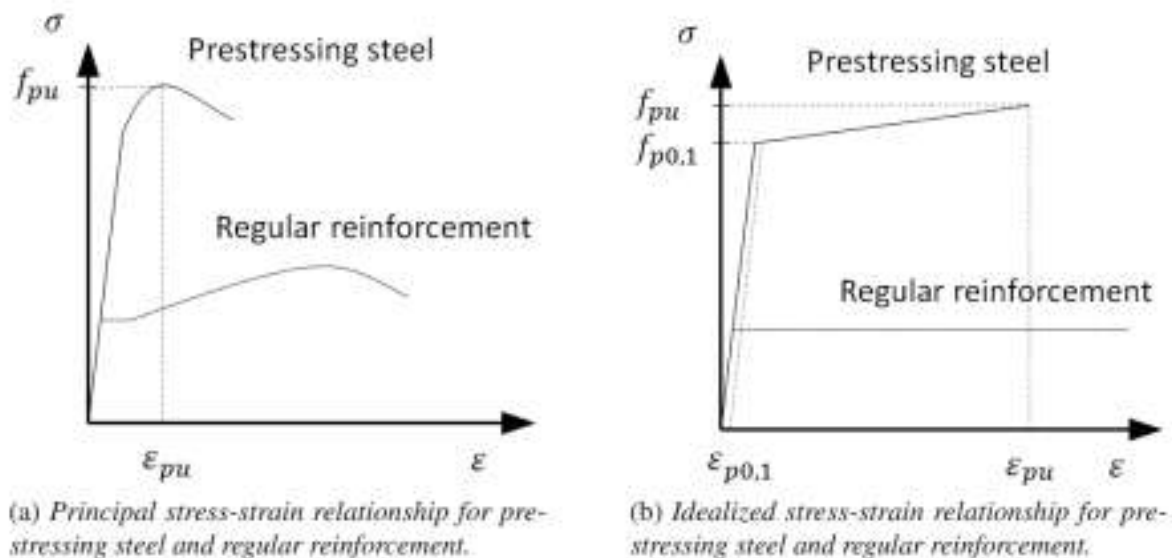


Figure 2-3 : Response of prestressing- and reinforcement steel (after Sacdirat, K et al 2007) .

In Figure 2.4a the load-displacement curve is demonstrated for a prestressed member subjected to an axial tensile force. For comparison the same curve for the reinforced member is put into Figure 2.4b. As mentioned earlier the prestressing effect delays the cracking of the member but does not affect the ultimate tensile resistance.

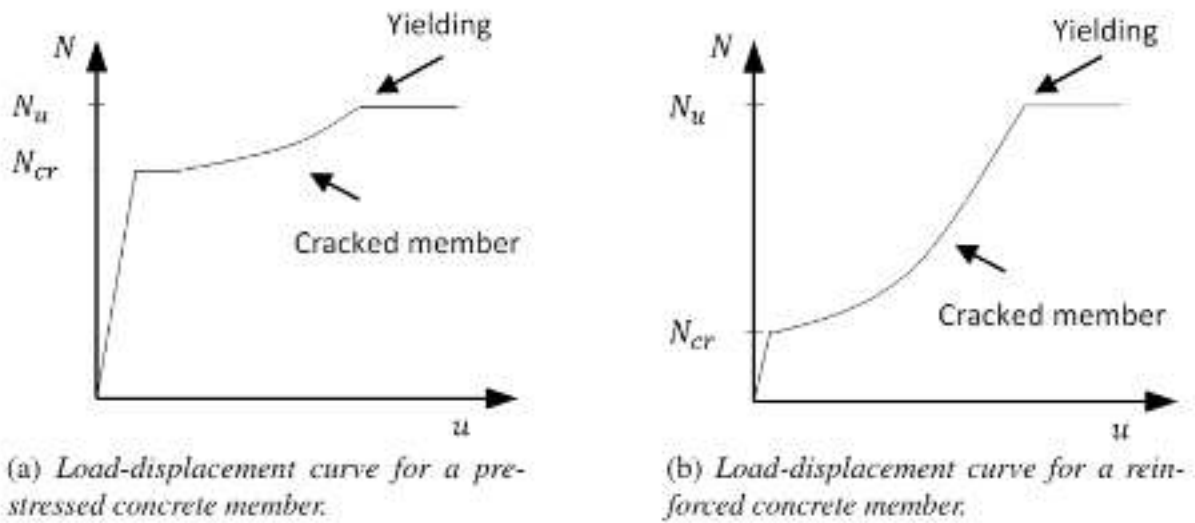


Figure 2-4: Load-displacement of prestressed- and reinforced concrete members subjected to an axial tensile force (after Sacdirat, K et al 2007).

Often when designing prestressed beam, the prestressing reinforcement is placed below the neutral axis, for simply supported beams in order to get positive moment acting upon the beam that will counteract the applied loads. The reinforcement can be placed at with a constant eccentricity, straight, or in a parabolic shape. Another results of this is a positive deflection will be present for unloaded beam, an example of load-displacement curve for an eccentric prestressed beam can be seen in Figure 2.5, where u_{pre} is the initial displacement due to prestressing.

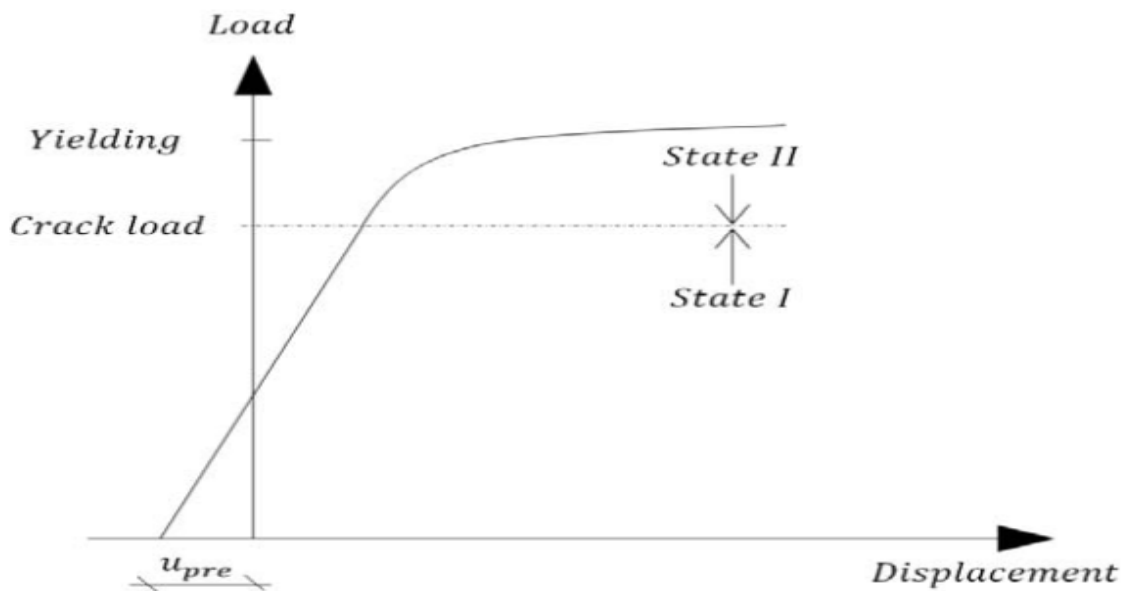


Figure 2-5: Load-displacement curve for an eccentric prestressed beam (after Sacdirat, K et al 2007).

2.3 Vertical dynamic behavior

2.3.1 Dynamic Properties of the Track

2.3.1.1 Receptance

One way to investigate the dynamic properties of a railway track is to subject the track with a sinusoidal force and then assess the receptance. The receptance is the quotient of the track deflection and the force put on the track, thus giving deflection in meters per Newton of the load. The receptance is the inverse of the track stiffness. Receptance functions show the vibration amplitudes of track structures as a function of vibration frequencies, in particular the deflection of a track structure under a unit load. The formal description of the receptance function is:

$$H_{\omega F}^2 = \frac{s\omega\omega(f)}{sFF(f)}$$

(1)

In which

$H_{\omega F}(f)$: complex transfer function from force to displacement (m/N)

$s\omega\omega(f)$: autospectrum of displacement (m^2s)

$sFF(f)$: autospectrum of the force (N^2s)

f: Vibration frequency(hz)

The dynamic equilibrium equation for this system yields:

$$C \frac{d\omega(t)}{dt} + K\omega(t) = \frac{-Md^2\omega(t)}{dt^2} + F(t)$$

(2)

By assuming the displacement function $w(t) = A_x e^{-i\omega t}$, The solution of this equation could be achieved:

$$\frac{\omega(t)}{F(t)} = \frac{1}{K - \omega^2 M - i\omega C}$$

Where,

K= Stiffness

M= Mass

C= Rayleigh damping coefficients

As the solution of this equation relates only to frequency if the mass, spring and damper properties are constant with respect to time, and linear with respect to force and displacement. Hence it can be called the

receptance function. It also can be expressed in a modulus $H(\omega)$:

$$H_{\omega F}(\omega) = \frac{1}{K} \sqrt{\frac{1}{\left(1 - \left(\frac{\omega^2}{\omega_e^2}\right)\right)^2 + (4\zeta^2 \omega^2 / \omega_e^2)^2}}$$

Where,

$H_{\omega F}(\omega)$: radial vibration frequency (rad/s) : $\omega = 2\pi f$

ω_e : eigen frequency (rad/s): $\omega_e = \sqrt{K/M}$

ζ : damping coefficient ratio: $\zeta = \frac{c}{2\sqrt{KM}}$

2.3.1.2 Resonance

A general description of the vertical dynamic behaviour of the track is introduced in order to understand the role played by each component. The presence of these components gives rise to several resonant frequencies, which are presented in Figure 2.6. It shows the frequency response of a periodically supported track due to a static load.

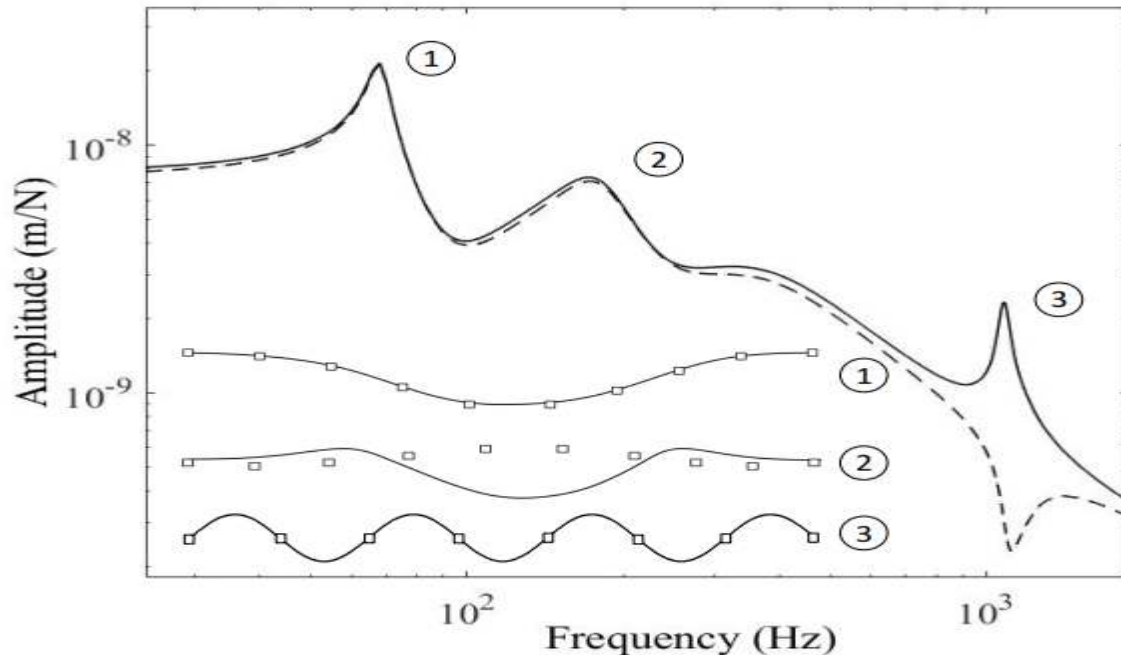


Figure 2-6: Track receptance at the exciting point. Mid-span excitation (—). Excitation above a sleeper (- -). The mode shapes are qualitatively represented.

The three resonances presented in Figure 2.6 are:

1. Sleepers and rail vibrating in phase: In this case the rail and sleepers act like the mass and ballast acts both as the spring and as a mass. Therefore, rail and sleepers are moving like a mass elastically connected to the ballast. This resonance normally takes place between 50 to 300 Hz.
2. Sleepers and rail vibrating out of phase: In this resonance the rail and sleepers act like independent masses connected by the railpads, which act as springs. Thus, the vibrating masses move in opposite directions. This resonance is found between approximately 200 to 600 Hz, mainly depending on the railpad stiffness.
3. Rail resonance: The frequency where this resonance occurs is called 'pin-pin' frequency. In this vibrating motion the movement is chiefly located in the rail, and the supports resemble rigid joints. It first happens when the wavelength of the rail bending waves is twice the sleeper spacing, which generally is around 1000 Hz. This vibration is poorly damped; since, the displacement is located in the rail, and its associated damping is mainly due to its own internal damping. The response to an excitation at this frequency strongly depends on exciting position. It is maximum at the mid of a span, and minimum above the sleeper, leading to a resonance and an anti-resonance, respectively. Excitation of the presented dynamic behaviour is mainly caused by the irregularities at the contact surfaces. The wavelength irregularities encompass a broad range, from 0.03 to even 2 m and, in turn, train operational speeds can cover from 10 to 300 km/h.

Therefore, the frequency range in which a track is excited is very wide, mainly from 1 to 2800 Hz. Other source of excitation is caused by changes of the foundation stiffness, which is known as parametric excitation. The most common example of this kind of excitation is due to the different flexibility between a point at the mid-span and another above the sleeper. It arises the so-called sleeper passing frequency, $f = V/l$, where V is the vehicle speed and l is the distance between sleepers. Other examples of varying flexibility are, transitions between ballast to slab tracks and changes on the rail sections and on the type of supports. These cases are very common in switches, crossing and stations.

2.4 Track modelling techniques

Track modelling has been a field of profound research during the last decades. Excellent reviews of track modelling can be found in (K. Popp, H. Kruse, and I. Kaiser, 1999) in which a first distinction is made between frequency and time domain modelling. The frequency domain modelling is normally addressed by analytical methodologies, because they entail a low computational cost. On the other hand, time domain modeling usually makes use of modal superposition and finite element methodologies, which can tackle more diverse cases including non-linearities.

Other major classification can be done depending on the rail modelling technique. In this respect, beam models based on Euler-Bernoulli and Timoshenko theories can be found. The Euler-Bernoulli theory neglects shear strain and rotatory inertia of the beam, therefore it is accurate for studies not exceeding a frequency around 500 Hz. On the contrary, Timoshenko beam theory takes into account both shear strain and rotatory inertia, and it is able to describe accurately vertical and lateral dynamics up to approximately 2500 and 1500 Hz, respectively.

Above these frequencies, Timoshenko theory is not accurate since the rail cross-section cannot be longer taken as non-deformable. Models describing the rail cross-section deformation can be found in (J. Gómez, 2006). With respect to the models that make use of the Timoshenko beam theory, analytical methodologies have been developed that account for the moving nature of the load and periodic foundation for the frequency domain. In spite of

their low computational cost, analytical methods require assumptions which are not met in a wide range of cases. Numerical techniques increase the computational cost, but they are able to perform simulations considering non-linear components, jointed tracks, sleeper voids, rail and sleeper lift-off, foundation transitions and finite length of supports.

2.5 Modeling of Ballast and Its Dynamic effect On Bridge

The numeric or analytic modeling of the railway track has been used together with field experiments to study its behaviour as well as its element characterization, its properties and also the vehicle-track-bridge interaction. Facing the desired goals, more or less detailed models can be used. The Ballasted Track can be modeled as a simple dead load, distributed over the deck, or by means of intermediate complexity models, in which the physical properties of the track are defined. 2D simplified models were presented on studies of previous authors, to represent the effect of the various elements of the track:

- **Non-vibrating ballast model:** (De Man, 2002 used a model in their studies which considers the rails represented as a beam with Euler-Bernoulli or Timoshenko behaviour and with such a length that the edge restrictions do not affect the structural behaviour. The sleepers are modeled as suspended masses connected to the beam, in the top, through parallel systems of spring-damper which represents the pads' properties, and to the subsoil/bridge, in the bottom, through parallel spring-damper systems which represent the ballast properties. In this model, the distance between elements is defined by the spacing between sleepers.
- **Vibrating ballast model:** (The Specialists' Committee D214 of the ERRI, 2001) presents a similar model to the one presented beforehand, but which considers the ballast modeled as suspended masses. These masses are connected to the sleepers, in the top, and to the subsoil/bridge, in the bottom, through parallel spring-damper systems which respectively represent the pads' properties and the connection between the ballast and the bridge subsoil.

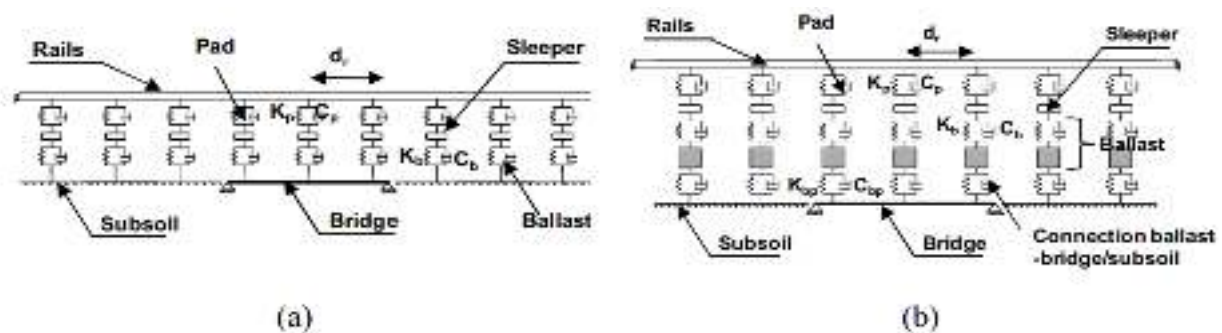


Figure 2-7. simplified models of ballasted track: considering the ballast without a vibrating mass (a) and considering the ballast as a vibrating mass (b).

(Zhai, 2004) presents various equations which allow the calculation of the vibrating mass and the vertical stiffness as a function of the geometry of the ballast layer and the distance between sleepers. The computation of each vibrating mass that corresponds to the influence of a half-sleeper is related to the attenuation angle (α) as presented in Figure 1 and expressed by the following equation.

$$M_b = \rho_b h_b [l_e l_b + (l_e + l_b) h_b \tan \alpha + (4/3) h_b^2 \tan^2 \alpha] \quad (3)$$

Where, ρ_b is the ballast density,

h_b is the depth of ballast,

l_e is the effective supporting length of half sleeper and

l_b is the width of sleeper underside.

The vertical stiffness for each vibrating mass of the ballast is computed by:

$$\frac{2(l_e - l_b) \tan \alpha E_b}{\ln(l_e/l_b)(l_b + 2h_b \tan \alpha)/(l_e + 2h_b \tan \alpha)} \quad (4)$$

Where, E_b is the elastic modulus of the ballast.

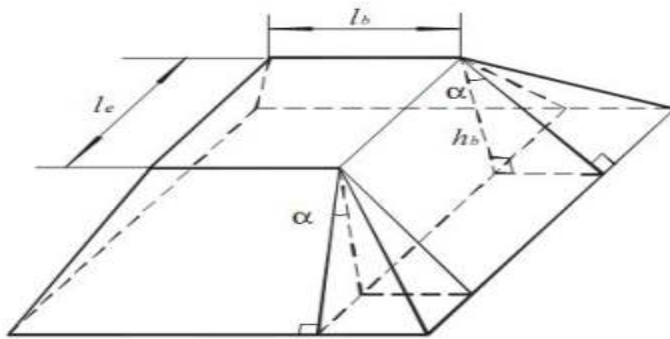


Figure 2-8: Model of the ballast under one rail support point

In (ZACHER et al, 2009) implement a 2D model of stiff ballast grains represented as balls with three degrees of freedom. The contact between the grains is then ensured through non-linear springs and viscous dampers. However, the 2D model implemented by (ZACHER et al, 2009) is not conceivable for the purpose of this thesis with a 3D finite element model.

Other studies show that the stiffness of the ballast is frequency dependent. For that, in (HERRON et al, 2009) consider a ballast stiffness range from 100 MN/m to 500 MN/m and model the ballast as discrete particles. In

contrast, in (REBELO et al, 2008) model the ballast layer as a plate connected to the bridge deck with springs and take into account only the shear stiffness of the ballast. These 2 studies end in the observation that the natural frequencies of a structure vary in line with the vibration amplitude. Besides, it's been shown that a rise in free vibration's amplitude end in the decrease of the first natural frequency of a bridge.

Then, in (LIU et al, 2008) implement a 3D finite element model and describe the ballast as solid elements, the sleepers as lumped masses and the rails as linear beams applicable boundary conditions are applied on the bridge longitudinal direction to simulate the continuity of the rails and also the ballast before and when the structure. The affiliation between the track and also the deck is ensured by a spring and damper system. During this study, the influence of the train model is investigated however all the models provide a good match with the experiment. Such a model for the ballast looks to produce fascinating results and it'll be more developed during this thesis.

(FINK et al, 2009) and (BATTINI et al, 2011) study the non-linear effect of the ballast superstructure on the bridge. Both studies introduce a 2D model, consisting of two beams: one modeling the bridge and the other modeling the ballast layer. Then, they study the interaction at the interface between these two beams. In (FINK et al, 2009) and (LIU et al, 2008), the effect of ballast is introduced through a non-linear longitudinal stiffness and the slip at the beam interface is taken into consideration into the ballast stiffness matrix. Good agreements between experimental and analytical results are found in each study. Such a model can also be implemented in a 3D FEM program.

(Bornet et al, 2013) achieved good conformity between measured and analyzed dynamic properties by using solid elements to model the ballast, 3D Thick (Timoshenko) Beam elements for the main beams, sleepers and rails and Thin (Kirchhoff) shell elements for the steel deck plates of a truss railway bridge in LUSAS. In this thesis the influence of ballast on the dynamic behavior of short span truss bridge is investigated. The thesis showed that ballasted track bridge has a lower natural frequency compared to unballasted track on the first four modes of vibration

(Lemma et al ,2017) also achieved a similar result between measured and analyzed dynamic properties by simulating 3D thick (Timoshenko) beam elements for sleepers, rail and beams and 3D solid model for ballast of steel railway bridge in ABACUS software. This method of modelling is used in this thesis as it is suitable for 3D FE analysis and delivers good results. In this study the influence of ballast and other track components on the dynamic behavior of steel bridge is investigated. The study showed that ballasted track bridge has a lower natural frequency compared to unballasted track on the first five mode of vibration. Moreover the thesis concluded that Neglecting the contribution of the ballast stiffness leads to lower natural frequencies that under-estimate the actual bridge stiffness.

These different works and conclusions about the train track bridge dynamic interactions are taken as a starting point of the thesis. No convincing model for the ballast superstructure has been implemented yet and as a result, the thesis will focus exclusively on this purpose and on the different parameters that can have a more or less significant influence on the ballast model and therefore, on the dynamic analysis of a bridge.

3. Methodology

3.1 Static Load Test

The aim of this test was to determine the actual deflections and stresses on the T-girder due to a standard load according to the China national code for testing RC T- girder bridges. To find out the mentioned parameters, a special five legged plate load is placed on the bridge in such a way that it would apply maximum stresses and deflections on the structure. A repetitive tests with different magnitude is conducted on the bridge to determine the actual structural behavior and basic parameters of the bridge. These include deflections, and stresses at particular points of interest on the bridge under static load. Five spots of interest will be assessed in the longitudinal direction: one each at 8m from the abutments/supports, one each at 12m from the abutment/support, and one at mid span. Finally the result will be used for the verification of model that is developed by FEM.

3.2 Finite Element Analysis

The finite element analysis (FEA) is a computing technique that is used to determine approximate solutions to boundary value problems. It uses a numerical method called finite element method (FEM). FEA uses the computer model of a design that is loaded and analysed for specific results, such as stress, deformation, deflection, natural frequencies, mode shapes, and so on. The T- girder ballasted railway track will be modelled and analysed as 3D using the finite element software ABACUS.

3.3 Analysis Type

1) Static Load Analysis

Static analysis can involve both linear and nonlinear effects and is applied to analyse static behaviour such as deformation due to a static load. A criterion for the analysis to be possible is that it is stable. A static step uses time increments, not in a manner of dynamic steps but rather as a fraction of the applied load. The default time period is 1.0 units of time, representing 100% of the applied load. The nonlinear effects are expected, such as large displacements, material nonlinearities, boundary nonlinearities, contact or friction.

2) Linear Eigen Value Analysis

Linear eigenvalue analysis is used to find out an eigenvalue extraction to determine the natural frequencies and respective mode shapes of the model for different type of track component combination. The most vital dynamic characteristics of railway bridges are their natural frequencies. Natural frequencies shows the extent to which the girder is sensitive to dynamic loads and are measured by the number of vibrations per unit of time. The unit of frequency is Hertz (Hz) which is the number of cycles executed per second. Extraction of the natural frequencies and mode shapes can be made by defining and executing a linear perturbation step in the steps module. The first 10 modes that has lowest frequency will be requested from the Lanczos Eigen solver in this step. The study will investigate how each track component affect the stiffness of the T- girder bridge by analyzing the following models.

- I. T- girder bridge alone
- II. T- girder bridge and ballast
- III. T- girder bridge, ballast and sleeper

IV. T- girder bridge, ballast, sleeper and spring rail

The selected methodology to follow in the research consists of four main stages. Each stage is properly developed and reported in this thesis.

- Computational model
- Model verification
- Transient analysis
- Sensitivity analysis

3.3.1 Computational model

The first step is to develop a computational representation of the bridge that behaves and responds as the actual bridge in the field. Literature review from Chapter 2 is used in this stage to design the model. The model is built using the software *ABACUS Structural Mechanics*.

3.3.2 Model verification

By applying static load analysis, it is possible to evaluate the accuracy of the model. If the model does not behave like the real bridge, the analysis and results generated through simulations are valueless.

3.3.3 Transient analysis

Once the model has been verified, the next action is to perform a transient analysis. The analysis is designed to investigate the response of the model under different structural conditions/case and track component combination. The simulations will show meaningful results that must be validated using actual data found from experiment.

3.3.4 Sensitivity analysis

The validated model from the first two stages will be evaluated using data from field tests. The model will be used to complete a sensitivity analysis and investigate the effect of having various densities, thickness, stiffness of ballast and boundary condition of the bridge.

4. Numerical Modeling of Ballasted RC T-Girder Bridge

Before dealing with the influence of ballast on the dynamic behavior of bridge it's important to validate the FEM model designed on ABACUS using static load experiment result.

4.1 FEM Model for the Ballasted Rc T-Girder Bridge Using Abacus

The finite element analysis (FEA) is a computational technique to extract approximate solutions to the partial differential equations that gives scientific and engineering applications, Finite element method employs various problems that use an integral of the differential equation over the problem domain rather than approximating the partial differential equation. This domain is subdivided into a various subdomains called finite elements (FE) and the solution of the partial differential equation is approximated with a simpler polynomial function on each subdivision element. These polynomials should be joined together to show approximate solution has an suitable degree of smoothness over the entire domain.

In fact, it is similar for any problem irrespective of its dimensions and degrees of freedom. The finite element method uses the following steps:

Pre-processing: In this step, the geometry is discretized into various numbers of small elements. These elements can be of different shapes and dimension. Each element is represented by number of points called nodes present in the element. Complete system of elements is known as mesh and the process of producing the elements is called mesh generation.

Preparation of elemental equations: In this 2nd step, algebraic equations are prepared for each element. A number of ways can be applied for this purpose. In this article, they are derived using direct FEM formulation, in which algebraic equations are obtained directly from the physics of the problem.

Assembly: In this 3rd step, the elemental stiffness equations are generalized to get a global system of equations.

Apply of boundary conditions: In this step, the generalized system of equations is modified by applying actual boundary conditions.

Solution: In this step, modified generalized system of equations is solved to get solution in the form of values of primary variables at nodes, like nodal deflection in axial rod problem and nodal displacement and slopes in beam/gider problem.

Post-processing: In this step, different types of secondary quantities are found from the obtained solution. For instance, stresses and strains are obtained from the computed nodal displacements in axial rod problem.

4.1.1 Material properties

The following material properties are used in the all track combination Abaqus models. The influence of variation of these physical parameters has been investigated for the ballast as discussed in section 5.

Table 4-1: Material property of track component and T- girder (From Material Specification of T-girder in Woldia/Haragebeya-mekelle Railway Bridge, 2014)

variables	Unit	Value
T-girder bridge		
modulus of Elasticity	Mpa	37000
poisson's ratio		0.2
mass density	Kg/m3	2500
T-flange Thickness	Mm	210
T-web Thickness	Mm	880
Ballast		
modulus of Elasticity	Mpa	80
poisson's ratio		0.16
mass density	Kg/m3	1800
Layer depth	Mm	450
Sleeper		
modulus of Elasticity	Mpa	37000
poisson's ratio		0.2
mass density	Kg/m3	2500
Spacing	Mm	600
Width	Mm	220
Thickness	Mm	180
Length	Mm	2500
Rails(UIC 54)		
modulus of Elasticity	Mpa	205000
poisson's ratio		0.3
mass density	Kg/m3	7937.681

4.1.2 Modelling of Bridge component

4.1.2.1 FEA Element Types used in the model

Elements fall into four major categories: 2D line elements, 2D planar elements, and 3D solid elements which are all used to describe geometry; and various elements which are used to boundary conditions application. For instance these elements may include gap elements to show a gap between two elements of geometry. Spring elements are applied to a specific spring constant for a specified node or set of nodes. Rigid elements are used to define a rigid relationship in a model. The geometry of elements applied in the model is beam element for the rail, spring element with spring constant for the rail pad and 3D solid element for other T-girder railway bridge components. Their detail simulation is shown below.

Beam Element

Beam elements are long and slender material which can be oriented anywhere in 3D space with three nodes. Beam elements are 6 degree of freedom elements which allows both translation and rotation on every end node. That is the major difference between truss and beam elements. The I J nodes show element geometry, on the other hand K node defines the cross sectional orientation. This is the way to differentiate between the strong and weak axis of bending for a beam. A constant cross section area is assumed. In the picture 4.1 below the beam shape is shown only for visualization; the element is the dark blue rod. The I J axis runs from the end to end node. K is shown vertically above the I-j axis or could be horizontally to the right of I.

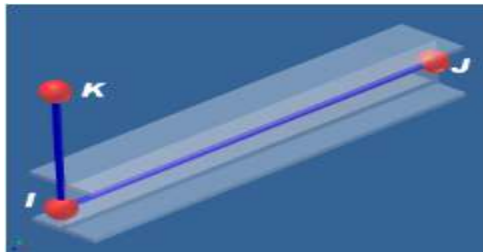


Figure 4-1: modeling of beam element

3D Tetrahedra Element, Wedge (3D Solid)

Tetrahedral elements can have 4, 5, 6, 7, 8, 15, or 20 nodes and support only translational Degree of freedom. They are normally applied to model solid materials in which plate elements are not suitable. One can usually describe either all tetrahedral, all bricks, or combination of both with some automatic mesh generators. This is the most usual, and frequently and the only element type that can be supported by automatic mesh generators. 3d tetrahedral elements can fit quite well for any "blocky" structures which are mostly fabricated from machine, casted, or forged fabricated parts. Structural and thermal bricks exist so that the similar model geometry can be applied for both the initial steady state heat transfer and subsequent thermal stress application.

4.1.3.1 Rail

Rails are linear elements that can be described typically by an infinite length. This allows rails to be modeled as beams. Rail has compression stiffness in the longitudinal direction and flexural stiffness in lateral and vertical directions. Rails also have shear stiffness even if it's usually neglected. Rails often modelled using either the Euler-Bernoulli or the Timoshenko beam theories. As most literatures suggest that several studies have shown that when the frequency of the vertical excitation force on the rail is below 500Hz, the Euler-Bernoulli beam model gives satisfactory results. However, in the case of higher frequencies, the shear deformation effect becomes increasingly essential and Timoshenko beam models give to accurate results. In this study all rails have been modelled as simple Euler-Bernoulli beams.

4.1.3.3 Ballast

As ballast materials possess voids within the material itself and also at the sleepers/ballast interface it deflects in a highly non-linear manner under vertical load. In spite of this, ballast beds are often modelled by discrete element or distributed viscous dampers and linear springs in the vertical direction. But thesis that was made by Lemma .m et.al (2017) and Lucie.B et. al (2013) modeled ballast as linear elastic 3D solid element and found a result close to reality on the study of dynamic analysis. Hence In this thesis, the ballast has been modelled as a linear-elastic element with a 3D solid element of specified Elastic modulus, poisonous ratio, and stiffness. The mass properties of a ballast bed are also included from the mass density definitions in the material properties that is specified on table 4-1.To represent the ballast layer, solid elements are generated and arranged on the T-girder bridge deck. The solid elements are meshed as a volume with tetrahedral elements

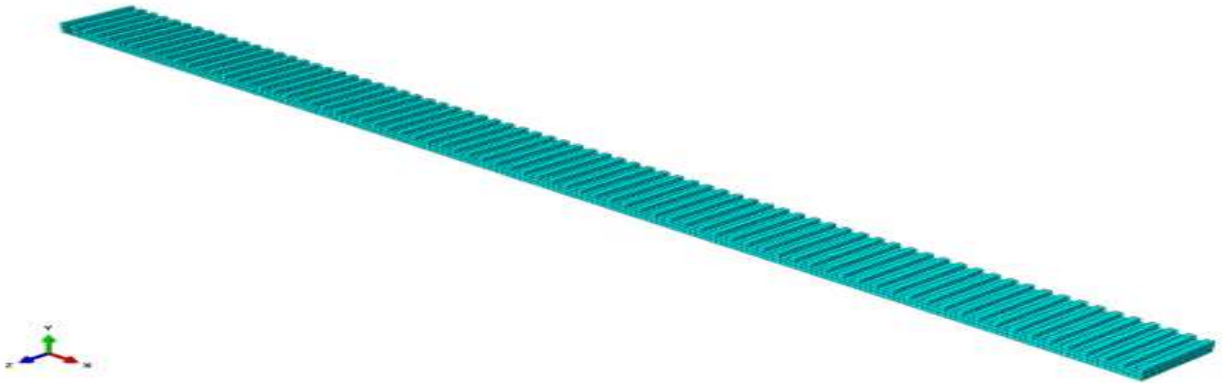


Figure 4-3: 3D Solid model of ballast

4.1.3.4 Prestressed T- Girder Bridge

The Bridge superstructure is composed of a two post tensioned T-girder which has a flange thickness of 210mm and a web thickness of 240mm length. The girder model is consisted of both solid and beam/truss element due to the characteristics of concrete and reinforcement respectively. Moreover the prestressing tendon is simulated like solid element with maximum stress of 33.1 MPa..

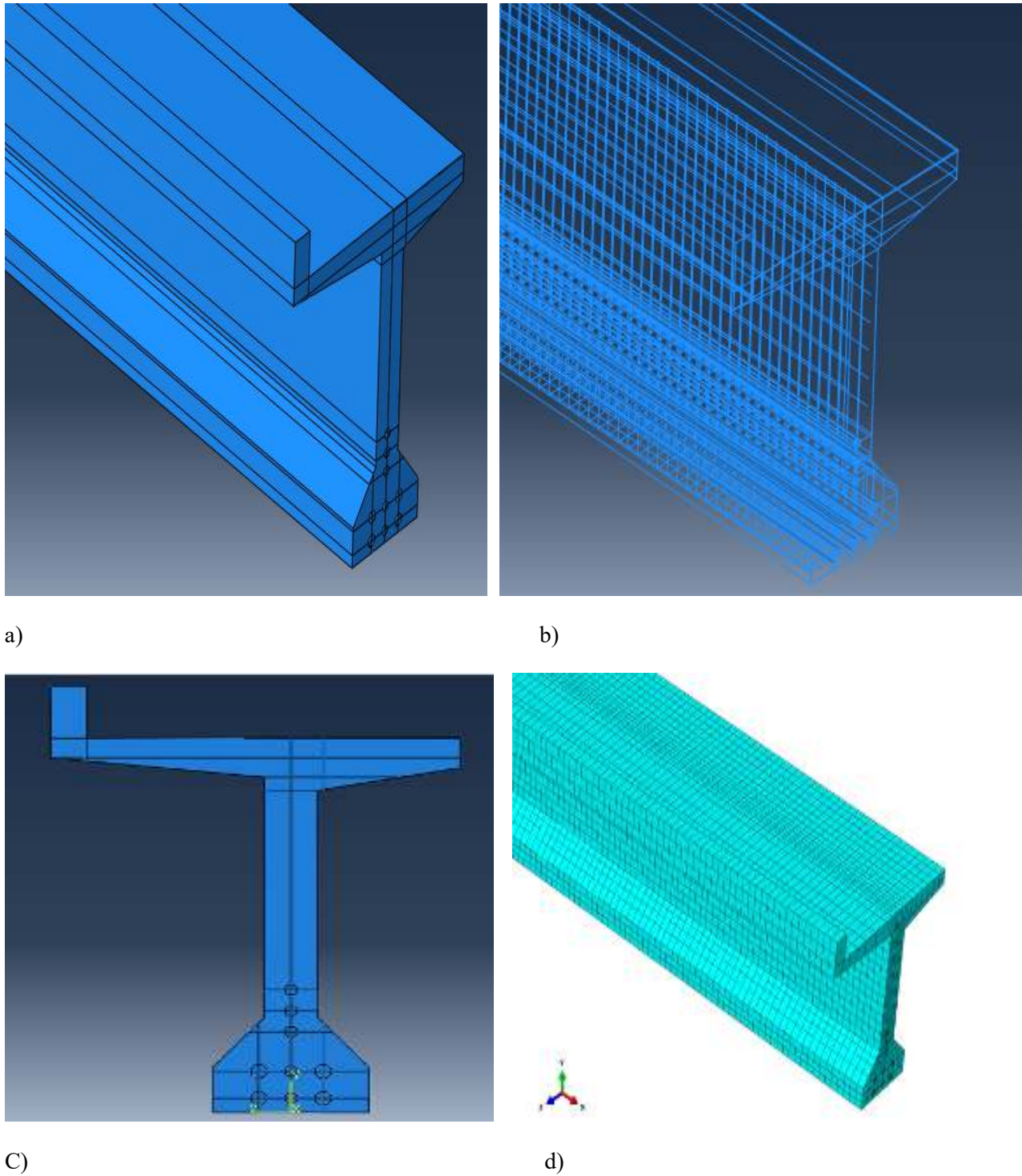


Figure 4-4: a) 3D solid, b) Reinforcement detail, c) Cross section and d) meshed model of prestressed T- girder

4.2 Validation and Eigen value analysis of the FEM model

The unballasted and ballasted finite element model has been developed based on the drawing in figure 4.5,4.6 and 4.7, in addition to observation from the Woldia/Haragebeya – Mekelle railway project. In order to make the model close to reality, the effect of some parameters like mesh size and interaction of prestressed tendon and concrete) has been tested by static load analysis. Finally the influence of each track component and support condition on the dynamic property of prestressed T-girder bridge is investigated by eigenvalue analysis.

The goal of this analysis is to obtain the natural frequencies of the T-girder Bridge accompanying to various eigenmodes for different types of track component combination will be applied. In this analysis the effect of ballast density (mass), stiffness, thickness, and support condition of the bridge on dynamic property of the T-girder railway bridge have been studied.

There are an infinite number of natural frequencies of structure with continuously disturbed mass. But when investigating the dynamic response of a bridge the lowest magnitude frequencies have many practical applications. The bridge structure picks and reacts to only the frequencies that are close to its own natural frequencies, when excitation forces are implemented to a system over a wide spectrum of frequencies. Due to this fact, natural frequencies have lot implications in dynamic analysis.

$$\omega_i = \sqrt{\frac{K}{M}} = 2\pi f_i \quad T_i = \frac{1}{f_i} \quad (5)$$

Where:- f_i = The notation for natural frequencies

The subscript $i = 1, 2, 3 \dots$ indicates their sequence.

Natural frequency is function of the natural circular frequency ω_i and the period of vibration T_i , as expressed in the equation above. The period signifies the time spent for one cycle.

4.2.1 Validation of the FEM model (Static load simulation)

The effect of various parameters on the stiffness of the T-girder bridge has been deeply investigated in this stage. Primarily, the effect of the mesh size has been studied and at the end, the desirable mesh size for each element has been applied to perform all the analyses. A maximum 5cm mesh size is used for the bridge in all 3 directions. This is due the fact that minimizing below this size is undesirable based on the static load test result.

However; the mesh size does not have significant influence on the results as long as realistic element size is chosen (Lucie.B et. al, 2013). Then, the effect of the nonuniform size of element has been investigated. For instance, the web thickness of the prestressed girder was made uniform unlike the real situation which varies on final 2m of span length. The difference observed from the static load analyses between uniform and nonuniform web thickness was insignificant: around 0.6%. Therefore uniform web thickness is used so that the model is simplified.

A resonant vibration frequency, or modal frequency, of a structure is a vibration often calibrated in hertz or cycles per second which can make a high relative magnitude of deflection. The resonant frequency of a structure is obtained when the frequency of applied dynamic load (in this case traffic applies a vibration in the

bridge) reacts with the output, or response frequency, of the bridge. A structure can have various numbers of resonant frequencies.

The relationship between a structure mass, stiffness and its resonant frequencies is shown by equation 6 above. The parameters that can influence most the magnitude of natural frequencies are mass and stiffness of the girder. At the beginning of the modeling the mass of girder was made to match with drawing, specification, and data gathered from precast yard. Static load test is used to verify strength (stiffness) of structures. Consequently the verification of stiffness of girder is thoroughly investigated by static load test which is discussed on section 4.2.2. The deflection the T-girder at the mid span is used as verification parameter. The prestressing tendon is modeled as embedded element and as a material which has high cohesive interaction with concrete girder. Modeling the tendon as embedded material give result more close to the result found in experiment.

In this study for validation purpose static load test was used for RC T-girder and detail dimension and specification of the girder is shown on the following topic. The static load test and the model result is shown on the experimental result section of the thesis.

4.2.2 Testing Of The Bridge

4.2.2.1 Brief description of the bridge under study

The bridge under study is a T-girder prestressed railway bridge located in Aware kebele on the track from Haragebeya to Mekelle, Ethiopia. Its physical coordinates is at 11.861°N, 39.671° E and is stationed at 11 km from haragebeya station. The free height under the bridge is just 12m.

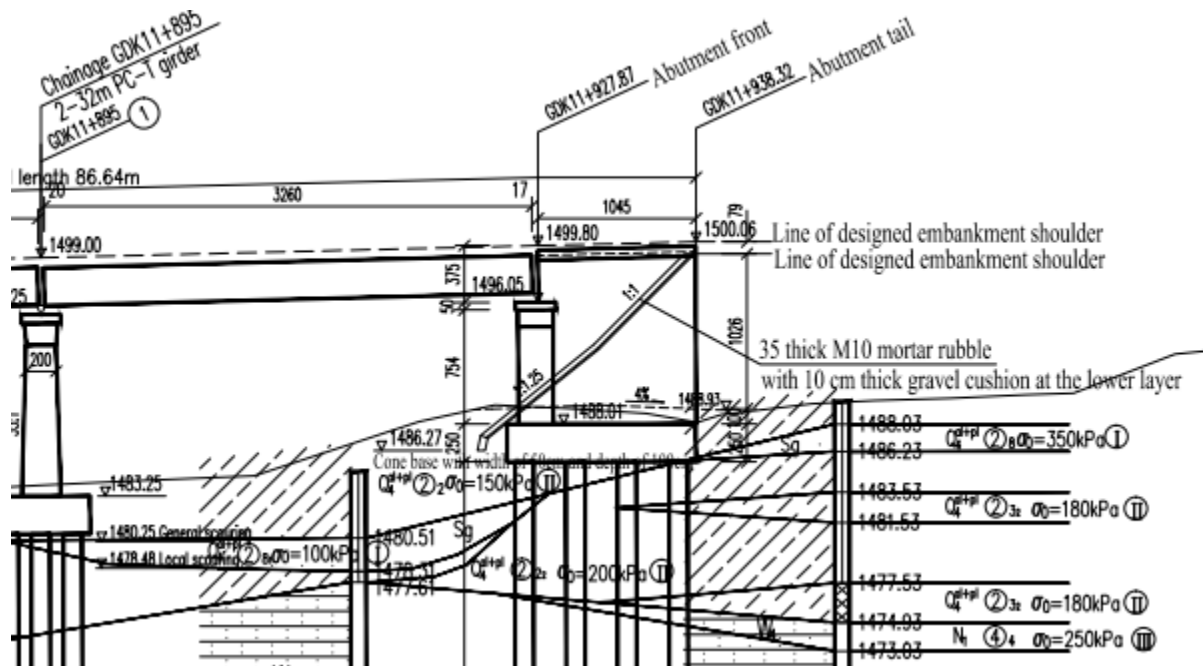


Figure 4-5: Location of the T-girder bridge

4.2.3 Geometry of the prestressed T-girder railway bridge

The aim of pre-stressing is to place the concrete structure under compression in the regions where load applied causes tensile stress. Tension caused by applied loads should primarily eliminate the compression induced by the pre-stressing tendon before it can crack the concrete structure. The girder is prestressed with maximum tensile stress of 33.1 MPa.

The girder has longitudinal length of 32.8m and a transverse both structural and non-structural width 2.3m and. HRB 335 and HPB 235 grade steel is used in all the structural elements of this bridge and Chinese railway class II construction was implemented. The bridge has an overall depth of just 2.5m with the web thickness 240mm and flange having a thickness of 210mm. ČSN 736201 requires a minimum ballast depth of 300mm below the sleeper's bottom. Two T- girder bridges located in parallel carry a single track positioned/situated in the middle of the transverse width of the two bridges. This track is supported by prestressed concrete sleepers that are placed at a spacing of 600mm. Two UIC 60 type rails are fastened on to these sleepers by Vossloh W14 fasteners.



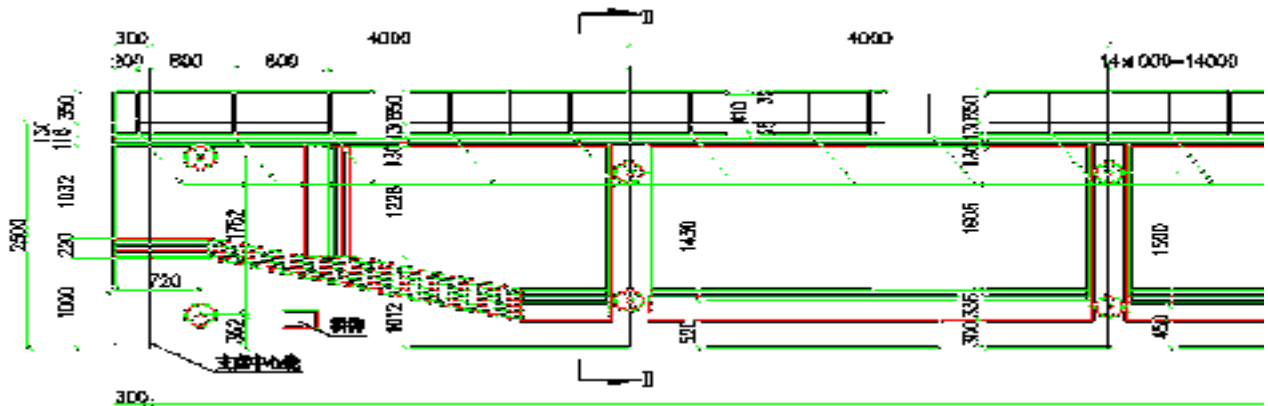


Figure 4-6: Longitudinal section of the T- girder

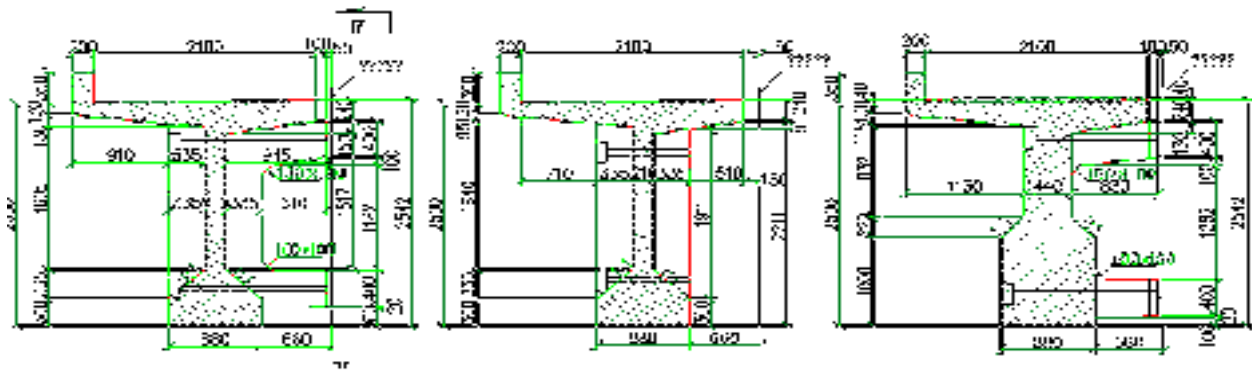
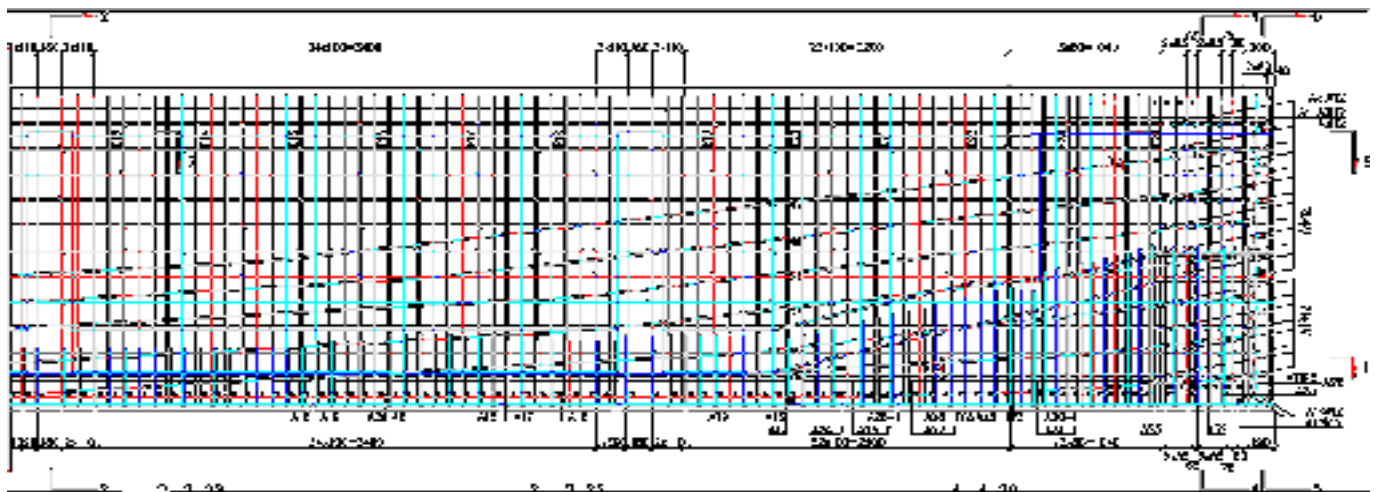


Figure 4-7: Cross-section of the T- girder



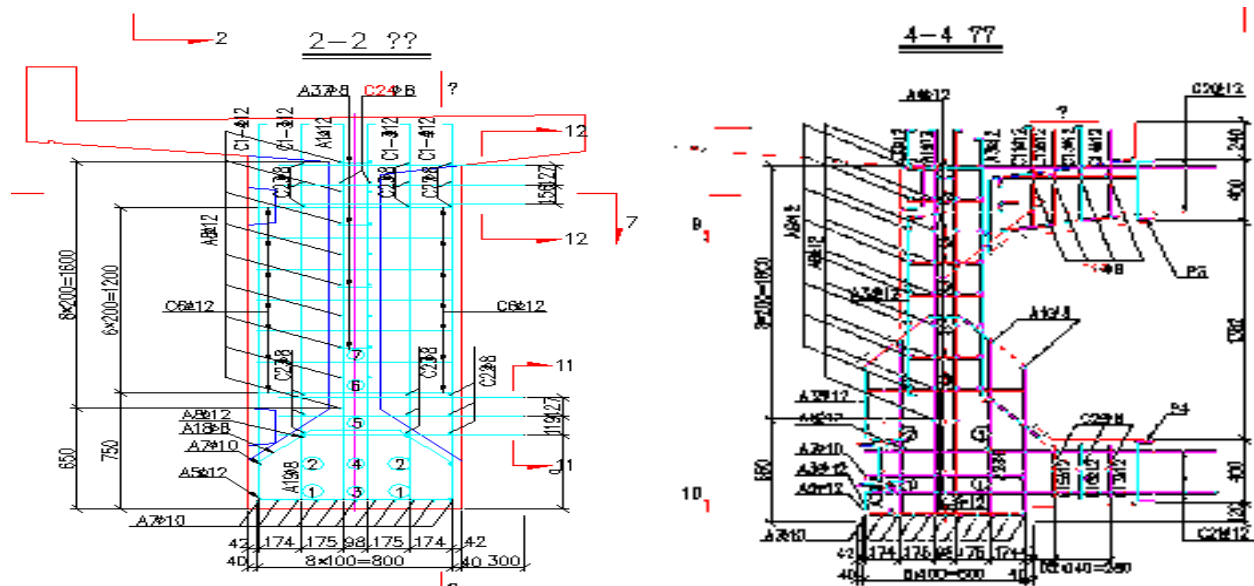


Figure 4-8: Reinforcement detail for prestressed T- girder bridge

4.2.4 Production and Erection

The new bridge was produced and assembled in a factory and brought over to the site where it was put to its current coordinates by a crane.

Phases of girder production process are as follows:

- 1) Preparing the mold,
- 2) Placing of reinforcement and duct,
- 3) Casting, compaction and curing of concrete,
- 4) Removing the mold,
- 5) Prestressing,
- 6) Storage



Figure 4-9: Production stage of the bridge



Figure 4-10: Erection of the bridge (On-site placement)

4.2.5 Experimental Model Loading

The experiment was done in Woldia/Haragebeya- Mekelle railway project head quarter at mechare. The test was done with presence of delegated quality control personal from contractor, consultant, client and me.

Five concentrated loads were applied at the mid-spans of the T-girder with spacing of 4m by electrohydraulic testing system of 2000 kN capacity, as shown in Figure 4-12. Static tests for observation of the elastic behaviour of the model were performed with 274.86 KN to 709.83KN value for each point. Displacements of the girder were measured at mid-span with flexometer deflection reader.

Structural behaviour has always been monitored until the effect of the load can be deem to be stable according stated in manual as described in TB/T 2092-2003 (Post-tensioned precast concrete simple-supported girder for railway bridge pro-stress).]. According to the standard, static load tests should be carried out with a static load that stays on the structure for at least 3 minutes for T-girder structures. Loading for 3 minutes if the load grade is less than 1.00 and loading for 5 minutes if the load grade is more than 1.00 for all load grades: static stop time shall be 20 minutes when $K_f = 1$ & 1.2. Static stop time (reflection restoration) shall be 10 minutes between the first cycle and the second cycle.

Both the Standard and the approved Method of Statement were made available before the test was carried out. However, in summary, the Static T-girder Load Test is about the application of a distributed load on the girder via five equally-spaced loading jacks and applied according to a particular loading sequence, after which the girder is investigated and computation made to make sure the effect of the load on the beam.

The deflection readings were monitored and checked during the experiment and obtained to be close to the calculated result. The deflection readings were calculated for the north and south side deflections and the average values used in the final measurement t of the deflection-span ratio for the beam.

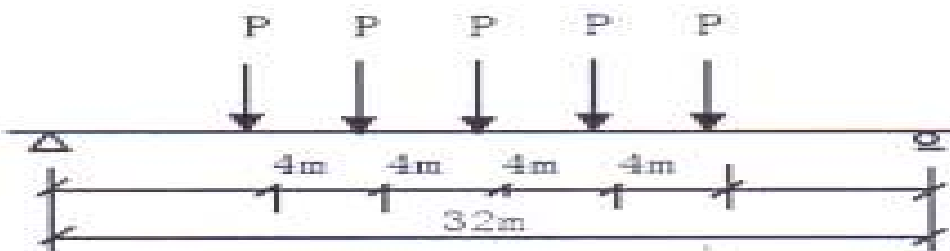


Figure 4-11: Load application on Prestressed T-girder bridge



Figure 4-12: static load test (On-site experiment)

Two Tests with two loading cycles were done in mechare (Head office of woldia/haragebeya –Mekelle Railway project) to determine the deflection at the mid span of the bridge, the result of the Experiment is shown on table 4.2 below.

Test -1																
First loading cycle								second loading cycle								
loading station	load grade	initial	base grad	0.6	0.8	static live	1	base grad	0.6	0.8	static live	1	1.05	1.1	1.1.5	1.2
	Loading (KN)		274.65	287.26	427.94	520.96	568.62	274.65	287.26	427.94	520.96	568.62	603.79	638.96	674.13	709.3
vertical displacement	Δ_0		2.54	2.54	2.64	2.69	2.72	2.55	2.57	2.7	2.73	2.77	2.77	2.77	2.77	2.8
	f1/2		15.96	16.76	23.77	28.6	31.71	16.49	17.22	24.43	29.13	31.91	33.84	35.47	37.46	39.4
	Δ_1		1.62	1.61	1.67	1.69	1.64	1.52	1.54	1.59	1.61	1.62	1.53	1.56	1.58	1.59
	$f=f_1/2-(\Delta_0+\Delta_1)/2$		13.88	14.685	21.615	26.41	29.53	14.455	15.165	22.285	26.96	29.715	31.69	33.305	35.285	37.205
Deflection value for mid span(mm)			13.445	14.25	21.18	25.97	29.09	13.82	14.535	21.655	26.33	29.083	31.06	32.675	34.655	36.575
Test-2																
First loading cycle								second loading cycle								
loading station	load grade	initial	base grad	0.6	0.8	static live	1	base grad	0.6	0.8	static live	1	1.05	1.1	1.1.5	1.2
	Loading (KN)		274.65	287.26	427.94	520.96	568.62	274.65	287.26	427.94	520.96	568.62	603.79	638.96	674.13	709.3
vertical displacement	Δ_0		2.05	2.11	2.39	2.56	2.67	2.3	2.32	2.55	2.68	2.75	2.79	2.85	2.91	2.99
	f1/2		15.64	16.53	23.87	28.95	32.27	16.55	17.29	24.83	29.7	32.58	34.59	36.31	38.38	40.42
	Δ_1		3.25	3.35	3.69	3.9	3.99	3.57	3.59	3.84	3.97	4.05	4.06	4.13	4.2	4.27
	$f=f_1/2-(\Delta_0+\Delta_1)/2$		12.99	13.8	20.83	25.72	28.94	13.615	14.335	21.635	26.375	29.18	31.165	32.82	34.825	36.79
Deflection value for mid span(mm)			13.73	14.54	21.57	26.46	29.68	14.045	14.765	22.065	26.815	29.61	31.595	33.255	35.255	37.22

Table 4-2: static load test result on the T-girder

Note: Δ_1 and Δ_2 are setting displacement in millimeters at each support and f1/2 is deflection at mid span of the girder

4.3 FEM Modeling of Static Load Test

Mesh sensitivity (convergence)

The load–deflection relation and the value of peak load converge to a stable state when mesh size (global seed size) is equal to or smaller than 5 cm. This observation is in agreement with the results found from the same material in static load tests (Section 4.2), which showed that load deflection relation of T-girder converges when element size of the T-girder is equal to or smaller than 5 cm.

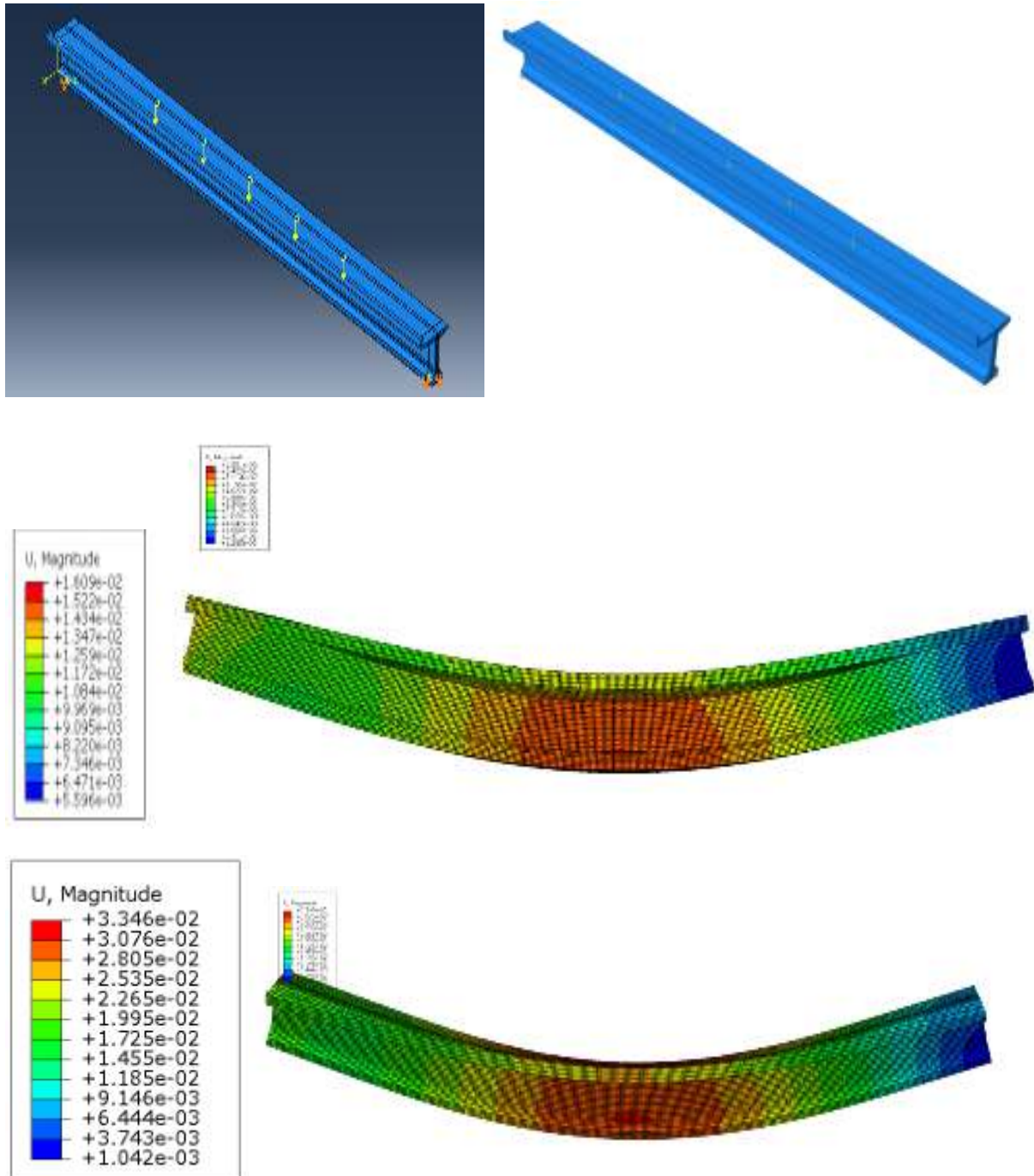


Figure 4-13: modeling of static load test by ABAQUS and its result

Load(kN)	Deflection		Difference(%)
	Experiment(mm)	FEM(mm)	
274.65	14.33	13.68	4.69
287.26	15.21	14.44	5.28
427.94	22.3	20.9	6.63
520.96	28.12	26.27	7.04
568.62	31.96	29.43	8.6
603.79	33.42	31.32	6.68
638.96	35.82	32.96	8.68
674.13	37.89	34.95	8.42
709.3	40.84	36.89	10.71

Table 4-3 : load deflection relation of static load model at mid span

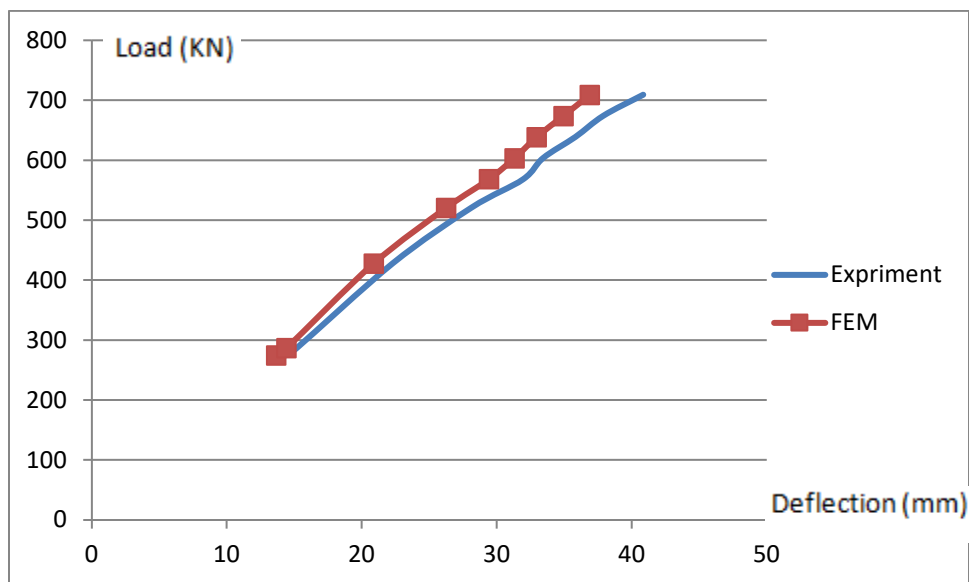


Figure 4-14: Deflection versus load graph for the experiment and model

It can be observed from Table 4.3 and figure 4.14 that the maximum variation of 10.71% is obtained by the model result in reference to experimental result which can be acceptable.

4.4 Analysis of Effect of ballast on the dynamic behavior of RC T-girder

4.4.1 ABAQUS Model Modal Analysis

Abaqus/CAE is a complete Abaqus environment that allows an easy, consistent interface for making, submitting, computing, and evaluating results from Abaqus/Standard and Abaqus/Explicit modeling. Abaqus/CAE is divided into modules, and every module is described in a logical characteristics of the modeling process; for example, defining the geometry of the structure, defining material properties of structure, and generating a mesh. By defining all obligatory data to each module, the model is built from which Abaqus/CAE generates an input data that can be sent to the Abaqus/Standard or Abaqus/Explicit analysis product. The analysis product executes the analysis, submit information to Abaqus/CAE to perform monitoring the progress of the job, and produces an output database. Finally, on the Visualization module of Abaqus/CAE (also licensed separately as Abaqus/Viewer) to read the output database and view the output of the analysis

The computation of the natural frequencies and mode shapes was done by defining and performing a linear perturbation step in the steps module. The first 10 modes that are not higher than a frequency of 20Hz were required from the Lanczos Eigen solver in this step. Boundary conditions that characterize how the structure is supported were defined in the Load module. The actual bridge bearing support condition as observed in Figure 4.11 was defined in all models. The assumptions for material property defined in table 4.1 are kept valid in all the following models.

In this sub topic the effect of ballast on the dynamic behavior of the bridge is investigated. Different cases (models) have been conducted to study the effect of track element on the bridge as it shown on the table 4.4 below. Hence by including the stiffness and mass effect of each track component on natural frequency of the bridge is investigated..

- I. T- girder bridge alone (T)
- II. T- girder bridge and ballast(TB)
- III. T- girder bridge, ballast and sleeper(TBS)
- IV. T- girder bridge, ballast, sleeper and spring rail(TBSR)

Moreover the effect of each material property (density, stiffness and depth) that characterize ballast is also investigated.

Model Component	Model/cases			
	T	TB	TBS	TBSR
T-Girder				
Element type	Solid 3D	Solid 3D	Solid 3D	Solid 3D
Elastic modulus	32Gpa	32Gpa	32Gpa	32Gpa
Ballast				
Element type		Solid 3D	Solid 3D	Solid 3D
Elastic modulus		80Gpa	80Gpa	80Gpa
Density		1800kg/m3	1800kg/m3	1800kg/m3
Sleeper				
Element type		Solid 3D	Solid 3D	
Elastic modulus		32Gpa	32Gpa	
Density		2500kg/m3	2500kg/m3	
Rail				
Element type				Beam
Density				7850kg/m3

Table 4-4 : Brief description of the models' parameter

Case-1 (Prestressed T-Girder Bridge Model Alone(T))

For comparison purpose, a simple model of the T-girder bridge neglecting the effect of stiffness of the track was prepared in ABAQUS modeling. However, both the contribution of stiffness and mass of the prestressed T-girder bridge have been considered in this case. The material properties used for this model are the default ones that is defined on section 4.1.2 of this study. Figure 4.15 shows the undeformed shape and meshed model of prestressed T-girder bridge. The first 10 natural frequencies were executed by running a linear perturbation analysis. The results are summarized in Table 4.5 and their shapes are presented on the annex part of the paper.

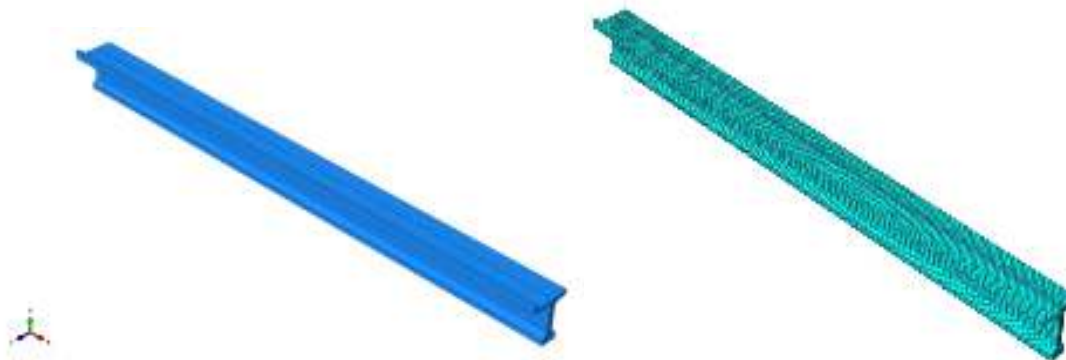


Figure 4-15: The undeformed shape and meshed model

Mode	Frequency(Hz)	Mode shape
1	2.511	longitudinal Bending
2	5.155	Transversal Bending
3	5.672	longitudinal Bending
4	7.264	Torsional
5	8.873	Torsional
6	9.369	Transversal Bending
7	11.09	longitudinal Bending
8	11.272	Transversal Bending
9	13.136	longitudinal Bending
10	14.145	Transversal Bending

Table 4-5: The first ten modes frequencies

Case-2 (Prestressed T-Girder and ballast Model Alone(TB))

In this model, both the stiffness and mass contribution of the ballast have been implemented. However, the contribution of the sleepers and the rails are neglected for comparison purposes. This means the stiffness and mass contribution of other track component is unaccounted in order to evaluate the effect ballast of ballast on the natural frequency of the T-Girder bridge. The material properties used for this model are the default ones that were defined in section 4.1.2 of this paper. Figure 4.16 demonstrates the undeformed shape of the meshed model of ballasted T-girder bridge. The ten natural frequencies were evaluated by running a linear perturbation analysis. The results are summarized in Table 4.6 and their shapes are presented in the figure 4.17 a and b below for better illustration.

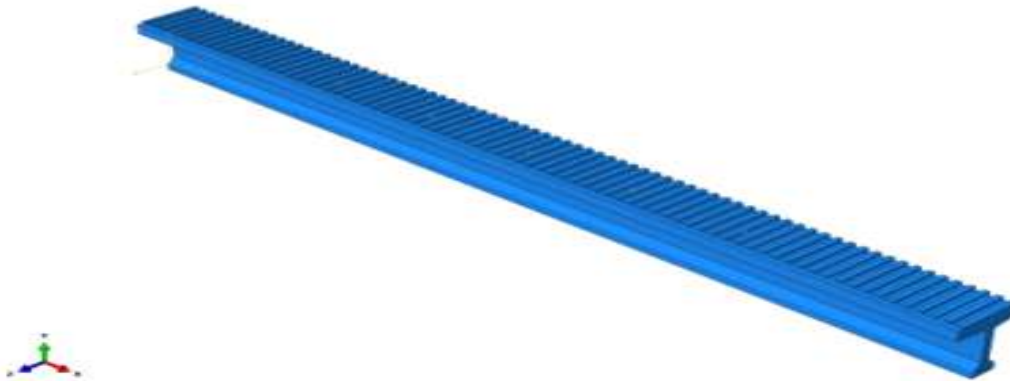


Figure 4-16: Undeformed shape of ballast and T-girder model

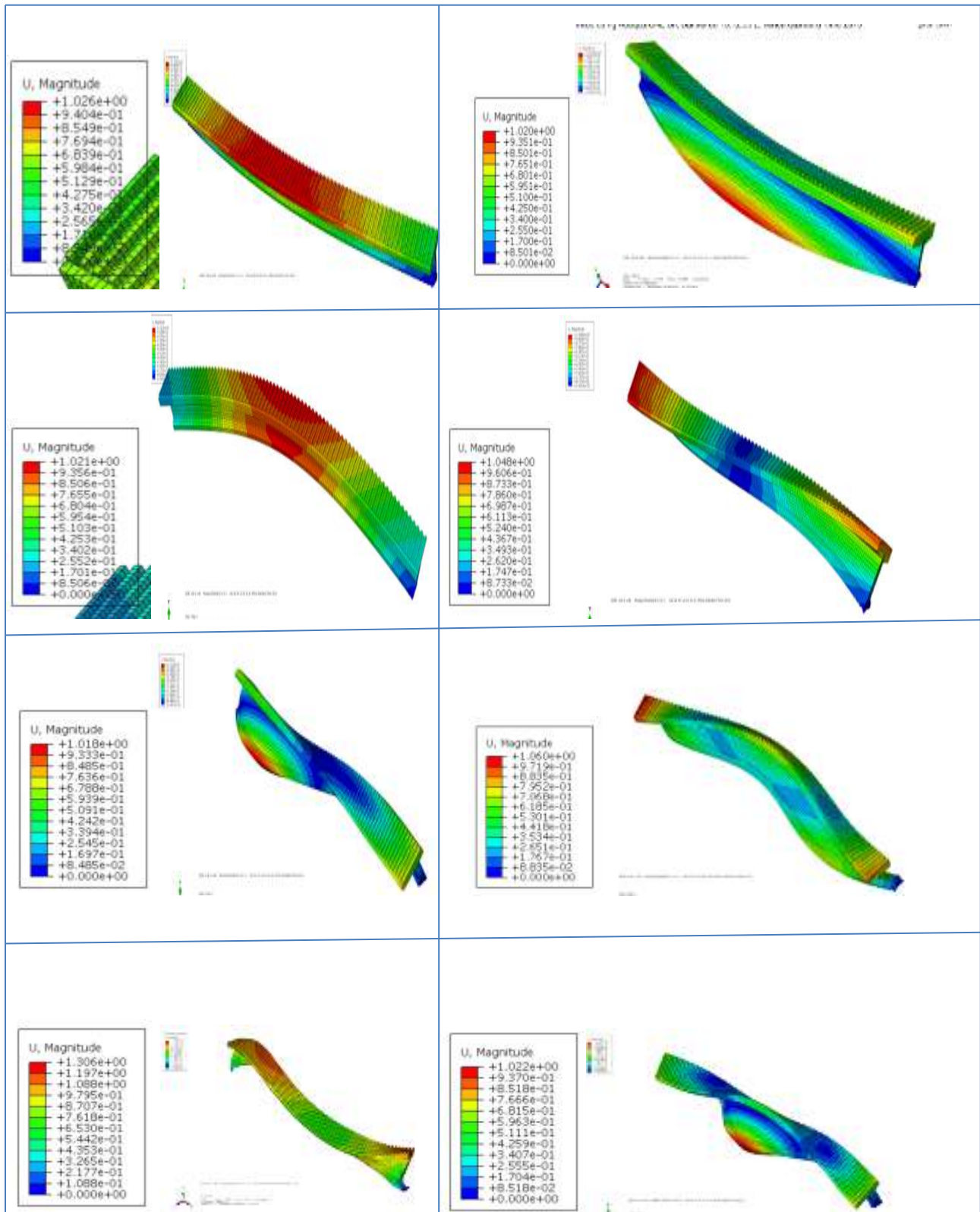


Figure 4-17 a: The first eight mode shapes of the model

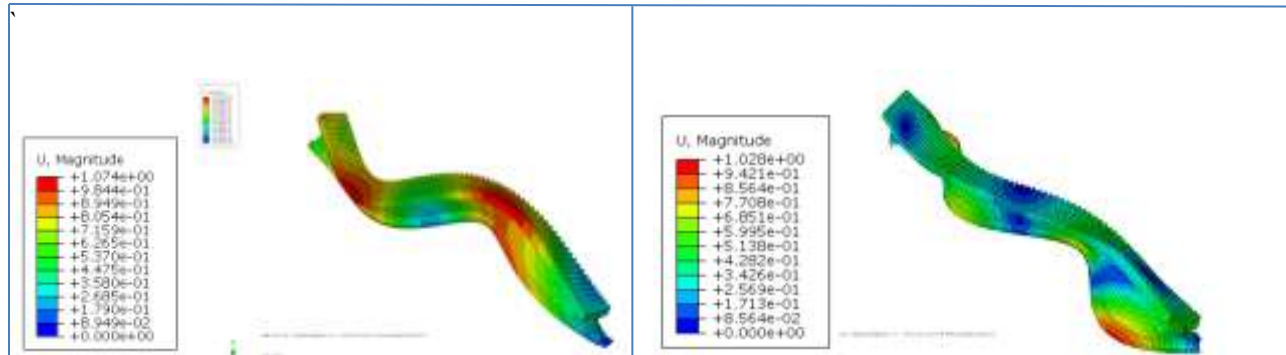


Figure 4-17 b: The 9th and 10th mode shapes of the model

Mode	Frequency(Hz)	Mode shape
1	2.155	longitudinal Bending
2	4.56	Transversal Bending
3	4.749	longitudinal Bending
4	5.984	Torsional
5	9.641	Torsional
6	10.262	Transversal Bending
7	12.877	longitudinal Bending
8	13.135	Transversal Bending
9	13.54	longitudinal Bending
10	13.849	Transversal Bending

Table 4-6: The first ten modes frequencies

Case-3 (Prestressed T-Girder, Ballast and Sleeper Model Alone(TBS))

In this model, both the stiffness and mass contribution of the ballast and the sleepers have been implemented. However, the effect of the rails is unaccounted. The material properties used for this model are the default ones that were defined in section 4.1.2 of this thesis. Figure 4.18 demonstrates the undeformed shape of the meshed model. The first ten natural frequencies were excuted by running a linear perturbation analysis. The results are summarized in Table 4.7 and their shapes are presented in the annex part of this thesis.

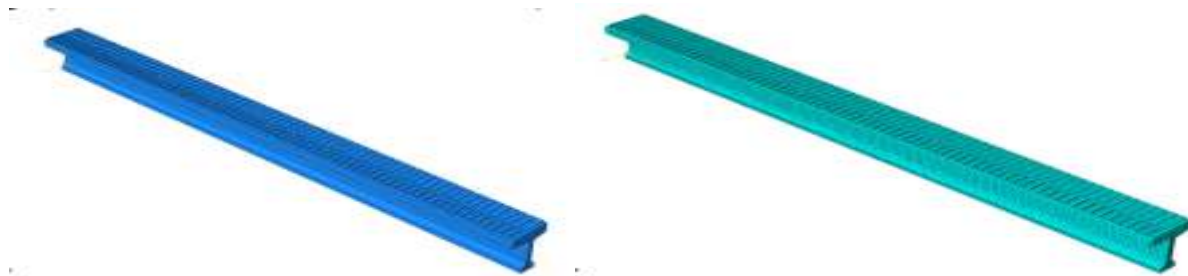


Figure 4-18: Undeformed shape and meshed sleeper,ballast and T-girder model

Mode	Frequency(Hz)	Mode shape
1	2.075	longitudinal Bending
2	4.446	Transversal Bending
3	4.57	longitudinal Bending
4	5.674	Torsional
5	9.505	Torsional
6	9.897	Transversal Bending
7	13.318	longitudinal Bending
8	13.48	Transversal Bending
9	14.969	longitudinal Bending
10	15.329	Transversal Bending

Table 4-7: The first ten modes frequencies

Case-4 (The Whole Bridge With Spring Rail To Sleeper Model (TBSR))

In this model, both the stiffness and mass contribution of the ballast, the sleepers and the rails have been implemented. The rails have been modeled as 3D beam element. The rail - sleeper connection has been designated a spring constant to show the relative resistances both in the vertical and longitudinal directions. The vertical stiffness is assigned for the resistance of the fasteners and rail-pads in vertical actions and 40MN/m² was applied taking in to account a unit length of the line for a unit deflection. Hence, a spring constant of 12kN/mm was applied at each node. Similarly for the longitudinal stiffness, the UIC recommended value of, 7.5kN/mm inside the bridge, as the ballast and sleepers have been defined, the only stiffness that needs modeling is that coming from the rail-pads and fasteners see Figure 4.19 below.

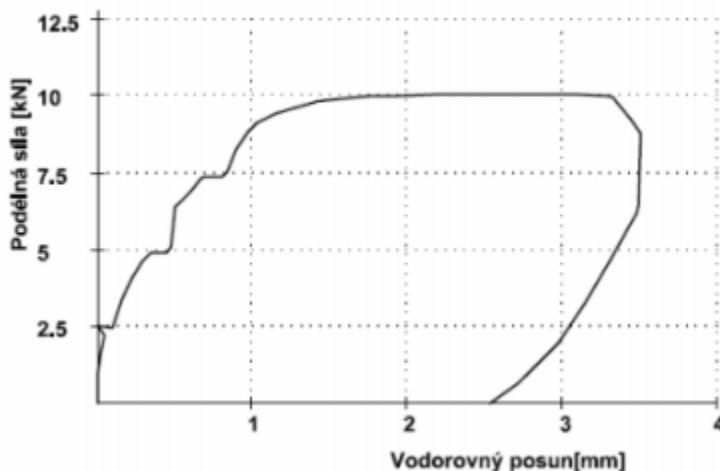


Figure 4-19 : Longitudinal resistance of Vossloh W14 Clamp Slk 14 fastner node

The material properties used for this model are the default ones provided in section 4.1.2 of this thesis. Figure 4.20 shows the undeformed shape and the meshed model and the rail support mechanism outside the bridge. The first ten natural frequencies were executed by running a linear perturbation analysis. The results are summarized in Table 4.8 and their shapes are presented in the annex part this thesis.

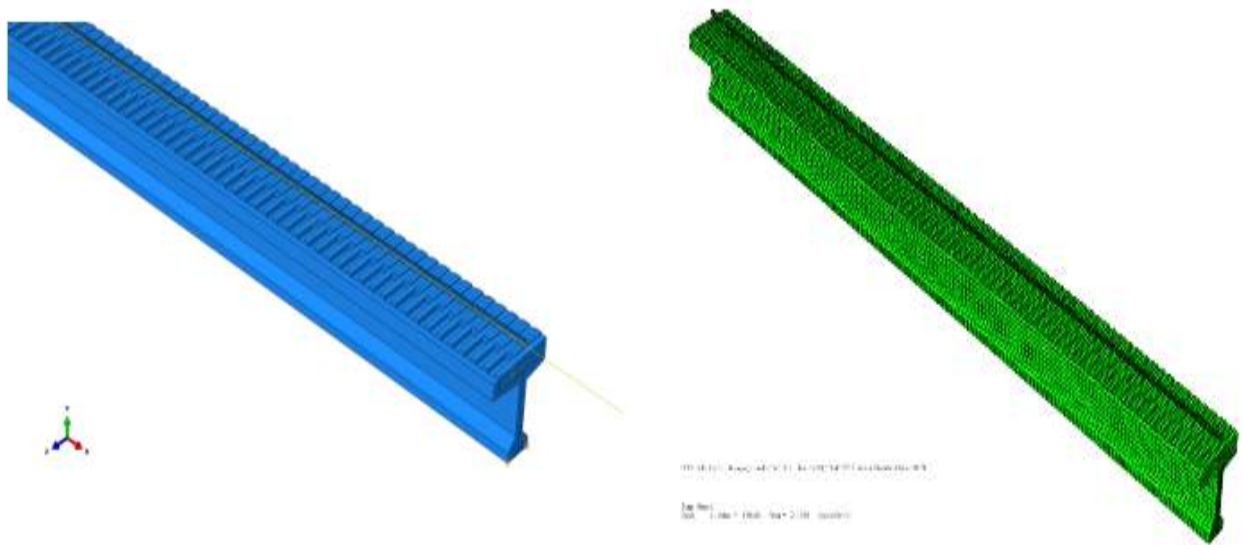


Figure 4-20: Undeformed shape and meshed Rail, sleeper, ballast and T-girder model

Mode	Frequency(Hz)	Mode shape
1	2.076	longitudinal Bending
2	4.442	Transversal Bending
3	4.592	longitudinal Bending
4	5.666	Torsional
5	9.509	Torsional
6	9.897	Transversal Bending
7	13.319	longitudinal Bending
8	13.515	Transversal Bending
9	14.972	longitudinal Bending
10	15.329	Transversal Bending

Table 4-8: The first ten modes frequencies

4.5 Finding

As it is discussed on section 4.4 four different models in Abaqus were investigated to find out the modal shapes and frequencies of the T-girder Bridge. A number of other models were made before arriving at these models. By implementing static load experiment all the refinement and modifications were made with aim of coming up with a model that best defines the actual bridge. Based on this, the effect of the stiffness and mass of each track component on the natural frequency of bridge is investigated

It can be seen from the table 12 below that model (T) where only the mass of the T-girder is included, estimated the natural frequency of the T-girder for the first ten modes of oscillation.

In model (TB), modifying the model by taking in to account the mass and stiffness of the ballast alone, resulted decrease in natural frequency of bridge 1-4th and 10th mode of oscillation in contrary an increase for 5-9th mode of oscillation. As it can be seen from table 12 and figure 28, the stiffness of the ballast is significant for the stiffness of the system for the higher frequencies unlike the lower frequencies. This is due to the fact the effect of stiffness of ballast is insignificant for 1st -4th mode of vibration compared to mass. On the other hand the mass of the ballast will affect the natural frequency of bridge on this mode of vibration. The opposite is true for the rest of mode of vibration of bridge. The effect of mass and stiffness of ballast on all types of mode of vibration of the bridge is explained in depth on section 5.

Additional modification of the model by taking into account the effect of sleepers resulted in a significant change on the natural frequencies in the model (TBS) from model (T) but slight difference from model (TB). The increase in the stiffness of the system for mode number 5-10 unlike for mode number 1-4 is due to the significant increase in the value of the elastic modulus (32GPa(concrete)) in the regions of the sleepers resuted to make the upper hand in guiding the natural frequencies over the relatively higher increase in mass density (1800kg/m³ to 2500kg/m³). In contrary, for mode number 1-4th the effect of mass of sleeper for 32m span bridge has higher effect in decreasing the stiffness of the system. The stiffness contribution of sleeper is insignificant for mode of vibration for the first four modes besides the increase in mass of system makes the structure to drop in natural frequency.

(TBSR), the last model in Abaqus, is a improvement of the previous model that involves rail and the use of springs to model the interface between the rail and the sleepers. Both the vertical and longitudinal stiffness are modeled. The computed frequencies and shapes for this model are in line with the model (TBS) results in almost all modes with the exception of 8. This is due the fact that the stiffness contribution of the high stiff rail for the system is equalized with mass effect of 32m highly dense rail material.

Mode	T	TB	% difference	TBS	% difference	TBSR	% difference
1	2.511	2.154	-14.217	2.075	-17.364	2.076	-17.324
2	5.155	4.561	-11.523	4.446	-13.754	4.442	-13.831
3	5.673	4.749	-16.288	4.571	-19.425	4.592	-19.055
4	7.265	5.984	-17.632	5.674	-21.900	5.666	-22.010
5	8.874	9.641	8.643	9.505	7.111	9.508	7.144
6	9.369	10.262	9.531	9.897	5.635	9.897	5.636
7	11.090	12.877	16.114	13.318	20.090	13.319	20.099
8	11.272	13.135	16.528	13.480	19.588	13.515	19.899
9	13.136	13.540	3.076	14.969	13.954	14.972	13.977
10	14.145	13.849	-2.093	15.329	8.370	15.329	8.370

Table 4-9: Summary of frequencies and modes of vibration from the numerical models

Frequency

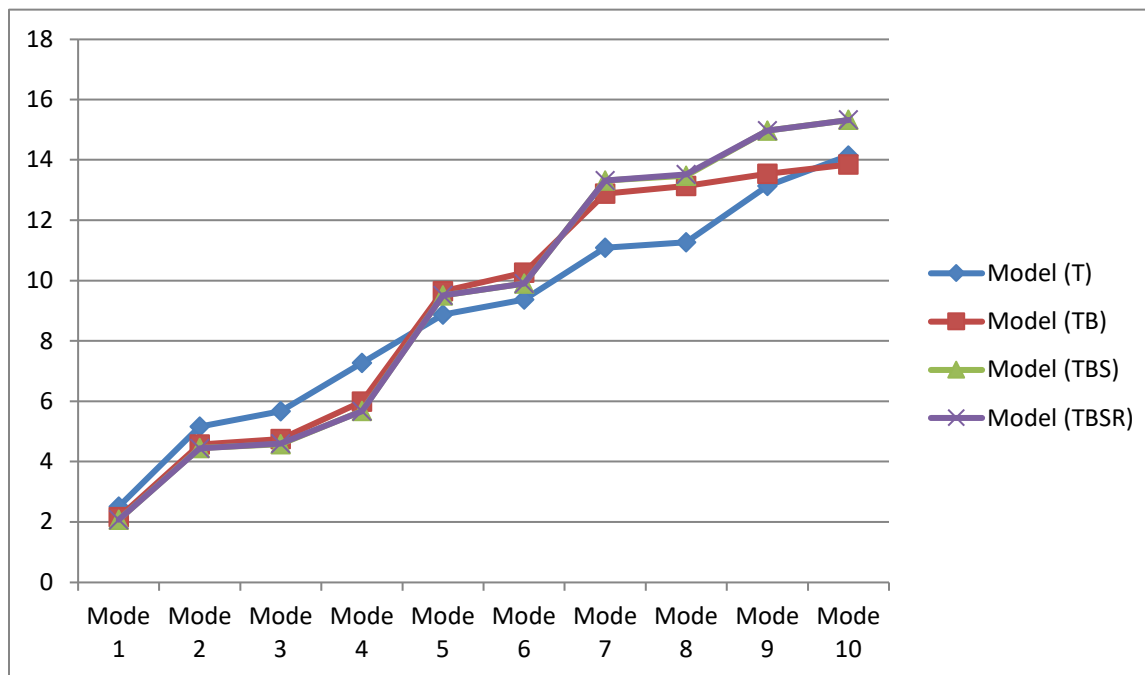


Figure 4-21: Frequency vs Mode graph for each model

5 Sensitivity Analysis

The effect of the mass, stiffness and depth of the ballast are studied in this section. For the purpose of this comparison, Model (TBSR) is chosen as a reference and a variation of the depth, mass and stiffness properties have been considered to assess their effects. The mode shapes remained the same as the reference case up on running analysis, however, changes were observed on the natural frequencies to a varying degree. Details of the observations are presented below.

Case	Parameters			
	stiffness	Density	Depth	Support Condition
Case0	80MPa	1800Kg/m ³	45cm	Pinned-Roller
Case1	40MPa	1400Kg/m ³	30cm	Pinned-Pinned
Case2	60MPa	1600Kg/m ³	40cm	
Case3	120MPa	2000Kg/m ³	50cm	
Case4	160MPa	2200Kg/m ³	60cm	

Table 5-1 Parameters to be studied on sensitivity analysis

5.2.1 Effect of stiffness of ballast

The significance of the variation of the ballast stiffness is evaluated by assuming three different sets of stiffness (strength) for the ballast material. The results are summarized in table 5.2. Three different ballast elastic modulus, thereby stiffness, values were computed. The modulus values ranged from 40MPa to 160MPa, which define the quality of the ballast from extremely bad to good. Comparative assessment of the results is shown in table 14 below.

Mode	TBSR	ballast = 40	% difference	ballast = 60	% difference	ballast = 120	% difference	ballast = 160	% difference
1	2.076	2.072	-0.207	2.074	-0.1	2.078	0.096	2.08	0.188
2	4.442	4.418	-0.536	4.433	-0.2	4.455	0.292	4.465	0.518
3	4.592	4.58	-0.257	4.587	-0.11	4.599	0.152	4.605	0.283
4	5.666	5.613	-0.935	5.645	-0.37	5.693	0.474	5.711	0.794
5	9.508	9.265	-2.561	9.424	-0.89	9.606	1.02	9.665	1.651
6	9.897	9.421	-4.81	9.791	-1.08	10.03	1.346	10.12	2.263
7	13.319	9.625	-27.74	11.537	-15.4	13.87	3.993	14.04	5.428
8	13.51	10.84	-19.79	13.12	-3.01	15.53	12.97	15.87	17.418
9	14.97	10.95	-26.88	13.276	-12.8	16.32	8.237	16.66	11.301
10	15.32	10.95	-28.59	13.407	-14.3	16.47	6.911	18.84	22.885

Table 5-2: Influence of ballast elastic modulus on vibration frequencies

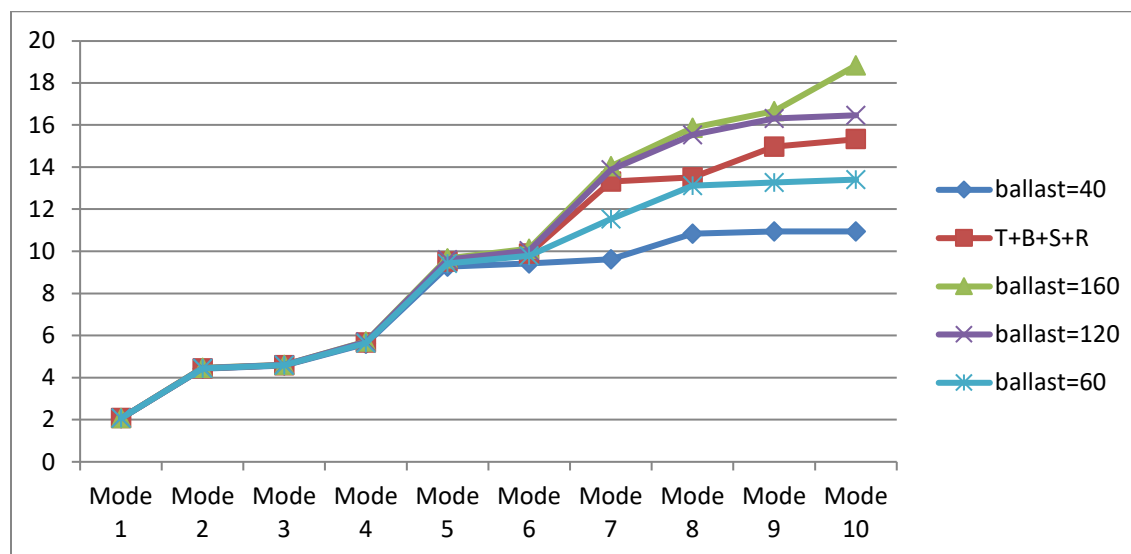


Figure 5-1: Frequency vs Mode graph for various ballast stiffness

Decreasing the stiffness of the ballast to a very low value of 40MPa (half the reference value), brought less than 1% drop in the lower frequency (mode 1-4) and 2.5 up to 28.59% decrease in the higher frequencies(mode 5-10). While increasing this value to 160MPa (Double the reference value) caused less than 1% increase in the lower frequencies (mode 1-4) mode and up to 22.88% increase in the higher frequencies modes (5-10). As it can be seen from the result, the stiffness of the ballast is significant for the stiffness of the system for the higher frequencies unlike the lower frequencies. This result shows that increasing the ballast stiffness made the bridge to be stiffer for dynamic load for higher modes.

5.2.2 Effect of ballast density

The significance of the variation of the ballast density were evaluated by assuming three different sets of unit weight (mass density) for the ballast material. The results are summarized in table 5.3.

mode	TBSR	ballast=1400	(%)difference	ballast=1600	(%)difference	ballast=2000	(%)difference	ballast=2200	(% difference)
1	2.076	2.141	3.136	2.108	1.518	2.045	-1.536	2.015	-2.948
2	4.442	4.549	2.409	4.494	1.157	4.394	-1.092	4.349	-2.094
3	4.592	4.716	2.703	4.653	1.311	4.533	-1.302	4.477	-2.504
4	5.666	5.916	4.412	5.787	2.091	5.552	-2.053	5.444	-3.918
5	9.508	9.704	2.061	9.614	1.103	9.384	-1.321	9.239	-2.829
6	9.897	10.29	3.93	10.074	1.757	9.759	-1.414	9.657	-2.425
7	13.31	14.04	5.376	13.768	3.261	12.64	-5.397	12.05	-9.535
8	13.51	15.1	11.757	14.131	4.359	13.26	-1.892	13.02	-3.64
9	14.97	15.6	4.188	15.288	2.067	14.53	-3.035	13.86	-7.4
10	15.32	16.3	6.328	16.187	5.301	14.56	-5.282	13.97	-8.859

Table 5-3 : Influence of ballast ballast density on vibration frequencies

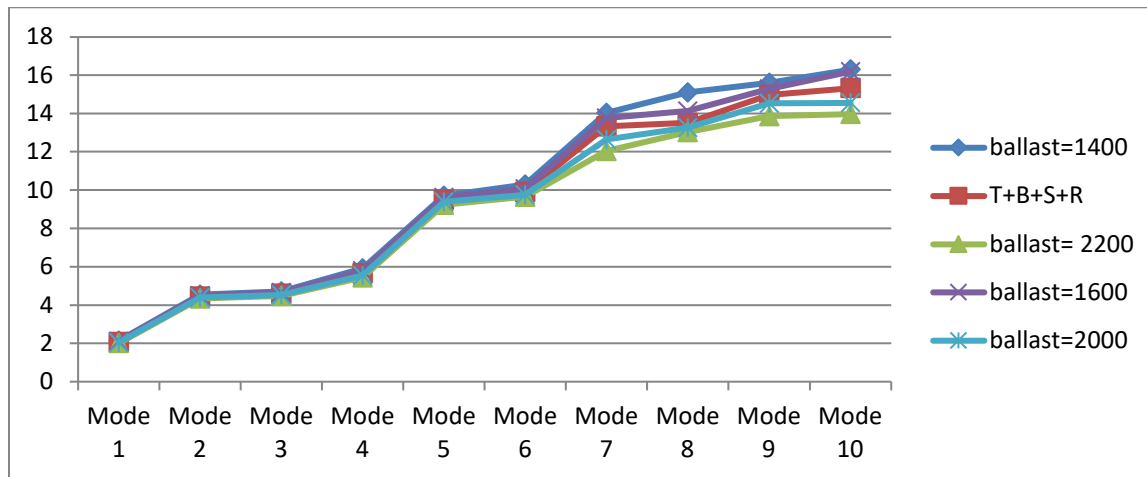


Figure 5-2: Frequency vs Mode graph for various ballast density

As expected, an increase in the mass results in a decrease in the natural frequency. An increase of the mass density by 400kg/m^3 resulted in 2.09 – 9.54% decrease in the natural frequency for the first 10 modes, inversely, decreasing the mass density of the ballast by 400kg/m^3 lead to increase by 2.14-16.30% for first ten modes of vibration. That means increasing the density of ballast made the structure to be less stiff for dynamic load as the natural frequency of the bridge shows how the structure is sensitive for dynamic load.

5.2.3 Effect of ballast depth

The significance of the variation of the ballast depth was evaluated by assuming three different sets of ballast depth for the material. The results are summarized in table 5.4.

Mode	TBS R	ballast=0.6m	% difference	ballast=0.5m	% difference	ballast=0.4m	% difference	ballast=0.3m	% difference
1	2.076	1.959	-5.636	2.0353	-2	2.121	2.134	2.203	6.132
2	4.442	4.211	-5.2	4.3614	-1.85	4.500	1.278	4.706	5.943
3	4.592	4.395	-4.29	4.5225	-1.54	4.714	2.593	4.883	6.331
4	5.666	5.203	-8.172	5.5046	-2.93	5.773	1.856	6.186	9.178
5	9.508	8.886	-6.542	9.3391	-1.81	9.541	0.345	9.768	2.735
6	9.897	9.527	-3.739	9.7312	-1.7	10.400	4.836	10.57	6.76
7	13.31	12.8	-3.897	13.187	-1	13.548	1.693	13.7	2.868
8	13.51	14.19	5.017	13.309	-1.55	14.073	3.968	14.77	9.293
9	14.97	14.28	-4.595	14.776	-1.33	14.982	0.067	15	0.174
10	15.32	15.37	0.248	15.098	-1.53	15.328	-0.006	15.32	-0.039

Table 5-4: Influence of ballast depth on vibration frequencies

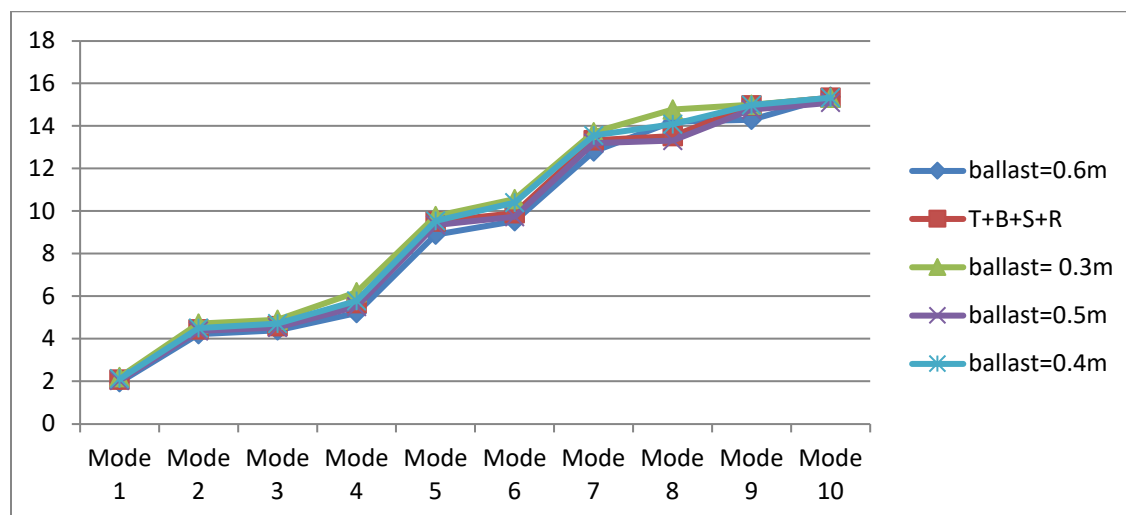


Figure 5-3: Frequency vs Mode graph for various ballast depth

Decreasing the depth of the ballast to a very low value of 0.3m, brought 0.17-9.18% rise in the first nine frequencies (mode 1-9) and the 10th mode is unaffected by the depth variation. While increasing this value to 0.6m caused 3.74-8.171% drop in the (1-7 and 9th) mode and 5.02% increase on the 8th mode. Generally, increasing the depth of the ballast made the structure to be less stiff for dynamic load. In choosing the depth of ballast for railway on bridge, it is essential to consider its effect on the dynamic behavior of the bridge.

5.2.4 Effect of support condition

Finally, the actual bearing support system used in the defined model were replaced to all pinned support system with the intent of evaluating the effect of such a change on the dynamic properties of the T-girder bridge. As the mass of ballast modifies the behavior of bearing of the bridge, Significant increase as high as 29.98% is observed in the frequency of the 3rd mode. This mode is highly influenced by the support conditions besides other modes showed a rise by 1.3-11.13% . However, the 2nd ,7th and 10th mode are unaffected by support.

Mode	TBSR	both pinned	% difference
1	2.076	2.307	11.127
2	4.442	4.448	0.135
3	4.592	5.969	29.987
4	5.666	6.209	9.583
5	9.508	9.821	3.292
6	9.897	10.026	1.303
7	13.319	13.321	0.015
8	13.515	13.731	1.598
9	14.972	15.326	2.364
10	15.329	15.476	0.959

Table 5-5: Influence of support condition of bridge on vibration frequency

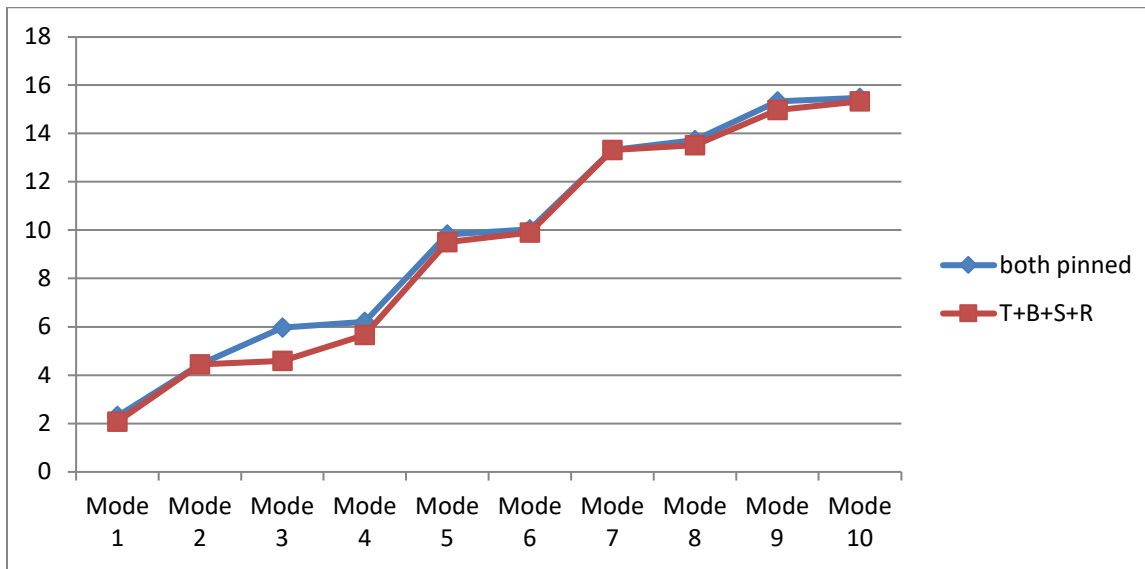


Figure 5-4: Frequency vs Mode graph for different bridge support condition

6. Conclusion and Recommendation

6.1 Conclusion

This thesis has studied the effect of ballast on the dynamic behavior of RC T-Girder Railway Bridge using a Finite Element Modeling (FEM) approach. A Mechanical characteristic of ballast layer with different depth, density, stiffness and support condition of the bridge are assessed. The influence of ballast on the dynamic behavior of the T-girder bridge has been numerically studied using natural frequency value found for four various track component combinations. Major findings of this thesis are highlighted as follows:-

1. According to the result obtained from static load test and numerical model, a fairly good output can be found by modeling RC T-girder Bridge and ballast as 3D solid element even in common structural analysis software such as ABACUS.
2. To analyze how much the ballast influence the stiffness of the RC T- girder bridge was investigated in this thesis by defining and making comparison between different 3D FEM models of the T-girder Bridge which define different structure and track component combination. This is essential as the natural frequency of structure shows how the structure is sensitive to dynamic load moreover it will show how much the structure is stiff for the dynamic load. Model that is composed of RC T-girder bridge and ballast alone showed a drop by (2.09-17.63) % in the natural frequency for vibration mode 1-4th and 10th (1st and 2nd degree longitudinal bending, 1st degree lateral bending and 1st degree torsion) and a rise by (3.07-16.52)% in the natural frequency for 5-9th (3rd and 4th degree longitudinal bending, 2nd and 3rd degree transversal bending and 2nd degree torsion) mode in comparison to ballastless model. Similar result was found for the first five mode of vibration on thesis that investigates the influence of track components on the dynamic behavior of steel bridge (Lemma et al ,2017). Moreover (Bornet et al, 2013) implement a 3D finite element model and describe the ballast as solid elements and found similar result when investigating the effect of ballast on the dynamic behavior of short span truss bridge. But the degree of influence of ballast varies from bridge to bridge. This is due to the significance of the mass and stiffness of ballast in comparison to the mass and stiffness of the bridge.
3. The two antagonistic parameters that define ballast which influence the dynamic behavior are also assessed. From the result it can be concluded that the stiffness of ballast is significant for higher mode of natural frequencies of the T- girder railway bridge. The effect of density and depth is similar. As the density or depth of the ballast increase the natural frequency of the bridge will decrease but their magnitude of influence on the natural frequency of the bridge will increase with the increase of the modes.

6.2 Recommendation

It is recommended that further research on the subject shall be considered,

- a. According to the sensitivity analysis the thesis tried to show the effect of density, stiffness and depth of ballast on the dynamic behavior of T-girder Bridge. Hence it is essential to consider the significance of the type of ballast material to be chosen in influencing the dynamic stiffness of the bridge.

- b. It would be preferable to compare experimental result of high-speed trains passing with a numerical dynamic response to study the effect of a moving train on the ballast model. However, the ballasted model proposed in this thesis may give output in very time consuming analyses for high-speed train applications.
- c. The whole conclusion obtained from this paper should be strengthened by other studies which assess the performance of different types of bridge. It may require to use a similar model than the one implemented in this thesis and check the effect the major parameters like density, depth, stiffness of ballast and support condition.

7. References

- 1) BATTINI, J.M., ÜLKER-KASUTELL M., (2011), *A simple finite element to consider the non linear influence of the ballast vibrations of railway bridges*, Department of civil and Architectural Engineering, KTH, Royal Institute of Technology, Stockholm, Sweden.
- 2) BUELL, D. C., (1914), *Ballast: a reprint of The Railway Educational Bureau's Track course Lesson*, University of Wisconsin.
- 3) C. RIGUEIRO, C. REBELO, L. S. D. SILVA AND M. PIRCHER, "Dynamic behaviour of twin single-span ballasted railway viaducts — Field measurements and modal identification," *Engineering Structures*, 2008.
- 4) COMPUTERS & STRUCTURES, INC, "Csi Analysis Reference Manual," Berkeley, California, USA, 2016.
- 5) DE MAN, AMNON P. *A survey of dynamic railway track properties and their quality*. Technische Universiteit Delft, Delft, 2002. PhD thesis.
- 6) DASSAULT SYSTÈMES' SIMULIA Corp., Abaqus/CAE User's Manual, 2012.
- 7) EN 1991-2, CEN (2003). Eurocode 1: Actions on structures – Part 2: Traffic loads on bridges
- 8) ERRI Specialists' Committee D214/RP 9. *Final Report - Rail Bridges for Speeds > 200 km/h*. European Rail Research Institute , Utrecht, 2001.
- 9) EUROCODE 1: *Actions on structures - Part 2: Traffic loads on bridges*, Brussels: European Committee For Standardization, 2002.
- 10) E. L. WILSON, "Three-Dimensional Static and Dynamic Analysis of Structures," Berkeley, California, USA, 2002.
- 11) FINK, J., MÄHR, T., (2009), *Influence of the ballast superstructure on the dynamics of slender steel railway bridges*, Institute of Structural Engineering, Department of Steel Structure, Vienna University of Technology, Vienna, Austria
- 12) HERRON, D., JONES, C., THOMPSON, D., RHODES, D., (2009), *Characterising the high-frequency dynamic stiffness of railway ballast*, Institute of Sound Vibration, UK. 78
- 13) J. M. PROENÇA, H. CASAL AND M. NEVES, "Effect of the type of track on the dynamic behaviour of high speed railway bridges," in *Computational Methods in Structural Dynamics and Earthquake Engineering*, Corfu, Greece, 2011.
- 14) LIU, K. REYNDERS, E., DE ROECK, G., LOMBAERT, G., (2008), *Experimental and numerical analysis of a composite bridge for high-speed trains*, Department of Civil Engineering, K.U.
- 15) L. BORNET, *Influence of the ballast on the dynamic properties of a truss railway bridge*, Stockholm, Sweden: Masters Thesis: Royal Institute of Technology (KTH), 2013.
- 16) LEMMA. M, *The impact of the ballast and track interaction on the dynamic behaviour of a short span steel bridge*: Czech Technical University in Prague
- 17) L. BJÖRKLUND, *Dynamic analysis of railway bridges subjected to high speed trains*, Stockholm: Royal Institute of Technology, 2004.
- 18) L. FRYBA, *Dynamics of Railway Bridges*, London: Thomas Telford Ltd., 1996.
- 19) L. BJÖRKLUND, *Dynamic analysis of railway bridges subjected to high speed trains*, Stockholm: Royal Institute of Technology, 2004.
- 20) REBELO, C., DA SILVA, L.S., RIGUEIRO, C., PIRCHER, M., (2008), *Dynamic behaviour of twin single-span ballasted railway viaducts*, Departments of Civil Engineering EST and FCT, Portugal.
- 21) UIC, UIC 774-3R: *Track/bridge interaction - Recommendations for calculations*, 2nd ed., 2001.
- 22) ZHAI, W.M., WANG, K.Y., LIN J.H., (2004), *Modelling and experiment of railway ballast vibrations*, Southwest Jiatong University, Chengdu, China.
- 23) ZACHER, M., BAEßLER, M., (2009), *Dynamic behaviour of ballast on railway bridges*, Germany.

8. Annex

8.1 static load test result on the T-girder



loading station	stage	the first loading cycle						the second loading cycle											
	load grade k	initial status	base grade Ka	0.6	0.80	static live load grade B1	1.00	initial status	initial status	base grade Ka	0.6	0.80	static live load grade B1	1.00	1.05	1.10	1.15	1.20	initial status
	loading Pk kN		274.65	287.26	427.94	520.96	568.62				274.65	287.26	427.94	520.96	568.62	603.79	638.96	674.13	709.30
vertical displacement at loading mm	Δ_0 Deflection	1.440	2.060	2.100	2.290	2.500	2.670	/	1.750	2.300	2.320	2.550	2.680	2.750	2.700	2.850	2.910	2.990	/
	$f_{1,2}$ midspan	1.480	15.640	16.000	21.870	28.930	32.270	/	2.070	16.850	17.200	24.820	29.710	32.580	34.550	36.510	38.380	40.420	/
	Δ_1 Deflection	1.000	3.255	3.350	3.680	3.900	3.990	/	1.250	3.570	3.590	3.880	3.970	4.060	4.060	4.130	4.200	4.270	/
$f = f_{1,2} - (\Delta_0 + \Delta_1) / 2$ deflection value (mm)		-0.740	12.890	13.600	20.800	25.720	28.940	/	-0.430	13.615	14.715	21.825	26.385	29.180	31.165	32.820	34.825	36.790	/
calculated deflection value for midspan mm		/	13.730	14.540	21.570	26.480	29.680	/	/	14.045	14.765	22.065	26.815	29.610	31.585	33.250	35.255	37.220	/
notes	1 Δ_0, Δ_1 are settling values of the supports at two sides; 2 Deflection measurement should be carried out before each cycle is coming to an end; 3 Average value of the deflection value of both sides of the girder shall be taken as the deflection value of each loading cycle.																		
observer name	Ethiopian RR railway Project of OGG						recorder	<i>[Signature]</i>	checker	<i>[Signature]</i>	reviewer	<i>[Signature]</i>							
loading station	stage	the first loading cycle						the second loading cycle											
	load grade k	initial status	base grade Ka	0.6	0.80	static live load grade B1	1.00	initial status	initial status	base grade Ka	0.6	0.80	static live load grade B1	1.00	1.05	1.10	1.15	1.20	initial status
	loading Pk kN		274.65	287.26	427.94	520.96	568.62				274.65	287.26	427.94	520.96	568.62	603.79	638.96	674.13	709.30
vertical displacement at loading mm	Δ_0 Deflection	1.880	2.540	2.540	2.640	2.680	2.720	/	1.640	2.550	2.570	2.700	2.730	2.770	2.770	2.770	2.770	2.800	/
	$f_{1,2}$ midspan	2.050	15.960	16.760	22.770	28.600	31.710	/	2.070	16.490	17.220	24.420	29.120	31.910	33.840	35.470	37.460	39.400	/
	Δ_1 Deflection	1.250	1.620	1.610	1.670	1.680	1.640	/	1.040	1.520	1.540	1.690	1.610	1.620	1.530	1.560	1.580	1.590	/
$f = f_{1,2} - (\Delta_0 + \Delta_1) / 2$ deflection value (mm)		0.435	13.880	14.685	21.615	26.410	29.570	/	0.630	14.450	15.165	22.285	26.960	29.715	31.680	33.300	35.285	37.205	/
calculated deflection value for midspan mm		/	13.445	14.250	21.180	25.935	29.095	/	/	13.825	14.535	21.865	26.330	29.085	31.060	32.675	34.655	36.575	/
notes	1 Δ_0, Δ_1 are settling values of the supports at two sides; 2 Deflection measurement should be carried out before each cycle is coming to an end; 3 Average value of the deflection value of both sides of the girder shall be taken as the deflection value of each loading cycle.																		
observer name	Ethiopian RR railway Project of OGG						recorder	<i>[Signature]</i>	checker	<i>[Signature]</i>	reviewer	<i>[Signature]</i>							

Table 8-1: Log Sheet Of Loading Time For Full Prestressed Girder Static Load Expriment (From laboratory report of woldia/Haragebeya-Mekelle railway project)

experimental stage	the first cycle								the second cycle														
	base grade Ka	0.60	0.80	static live load grade Kb	1.00	static live load grade Kb	base grade Ka	initial status	initial status	base grade Ka	0.60	0.80	static live load grade Kb	1.00	1.05	1.10	1.15	1.20	1.10	static live load grade Kb	base grade Ka	initial status	
standard loading time	3min	3min	2min	3min	20 min	1min	1min	10 min	/	3min	3min	3min	3min	5min	5min	5min	5min	20 min	1min	1min	1min	/	
start time of loading	14:35:33	14:41:13	14:46:18	14:52:23	14:56:28	15:14:39	15:15:28	15:17:01	/	15:37:56	15:41:44	15:46:06	15:51:01	15:55:24	16:01:42	16:09:26	16:14:11	16:20:02	16:41:12	16:42:56	16:44:55	/	
end time of loading	14:39:12	14:44:20	14:49:19	14:55:25	15:16:36	15:15:52	15:16:39	15:27:12	/	15:40:59	15:44:55	15:49:22	15:54:11	16:00:32	16:06:56	16:13:39	16:19:21	16:40:08	16:42:23	16:44:07	16:46:10	/	
actual loading time	0:03:08	0:03:07	0:03:01	0:03:04	0:20:08	0:01:13	0:01:11	0:10:11	/	0:03:03	0:03:11	0:03:16	0:03:10	0:05:08	0:05:14	0:05:13	0:05:10	0:05:10	0:33:08	0:01:11	0:01:11	0:01:15	/

8.2 Mode Shape Frequency values of Each FEM model

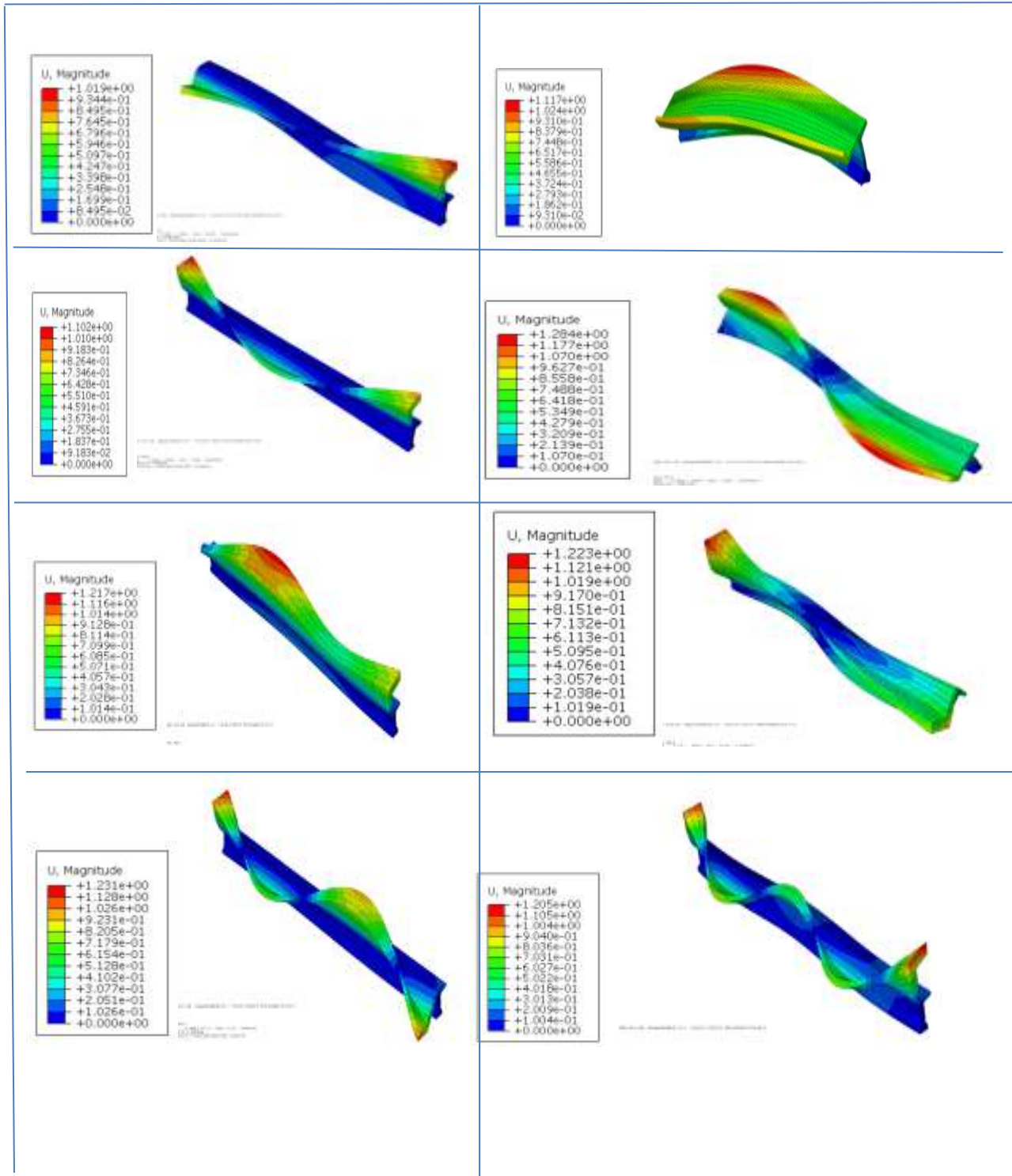


Figure 8-1: The first eight mode shapes of the model (Case1)

Frame

Index	Description
0	Increment 0: Base State
1	Mode 1: Value = 248.91 Freq = 2.5110 (cycles/time)
2	Mode 2: Value = 1049.1 Freq = 5.1550 (cycles/time)
3	Mode 3: Value = 1270.3 Freq = 5.6725 (cycles/time)
4	Mode 4: Value = 2083.5 Freq = 7.2647 (cycles/time)
5	Mode 5: Value = 3108.5 Freq = 8.8735 (cycles/time)
6	Mode 6: Value = 3465.8 Freq = 9.3696 (cycles/time)
7	Mode 7: Value = 4855.7 Freq = 11.090 (cycles/time)
8	Mode 8: Value = 5015.7 Freq = 11.272 (cycles/time)
9	Mode 9: Value = 6812.3 Freq = 13.136 (cycles/time)
10	Mode 10: Value = 7898.8 Freq = 14.145 (cycles/time)

Figure 8-2: The first ten natural frequencies of the model (Case1)

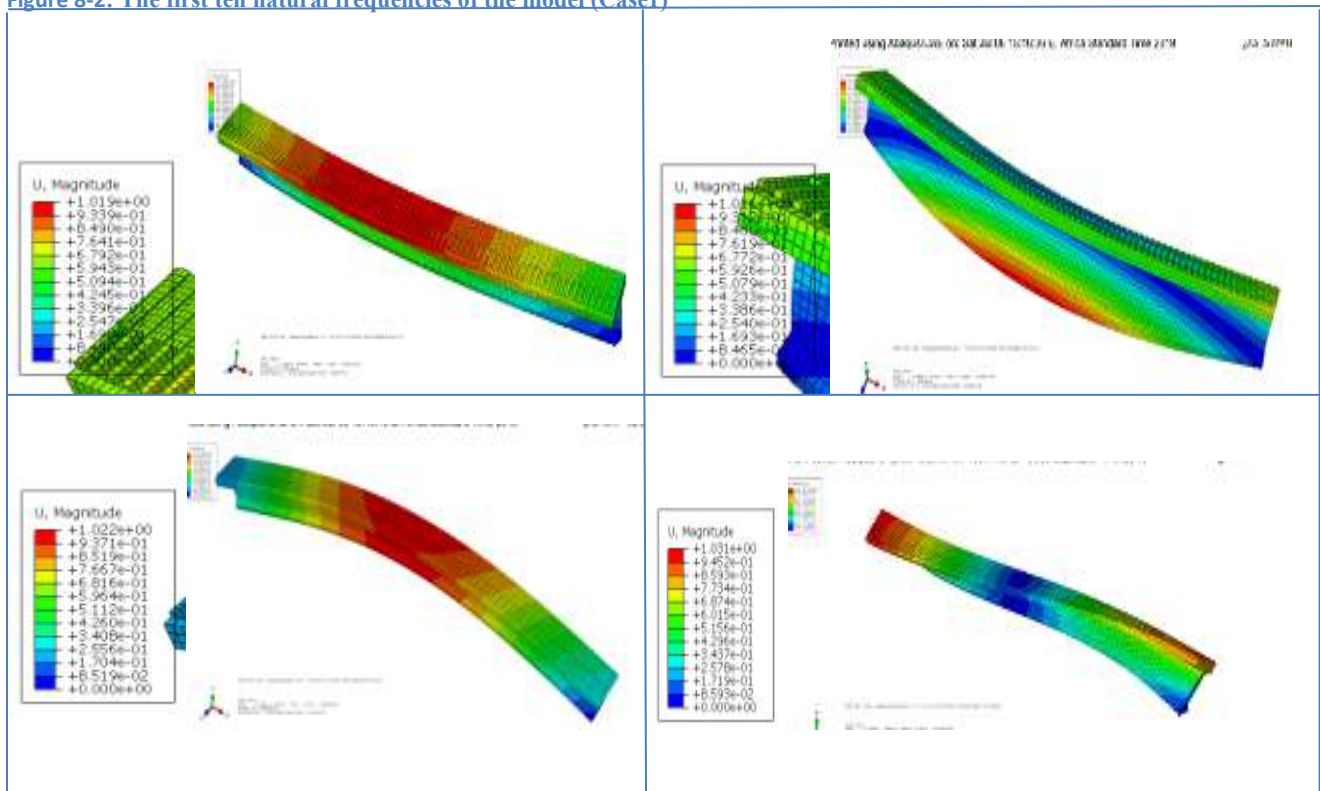


Figure 8-3: The first four mode shapes of the model (Case3)

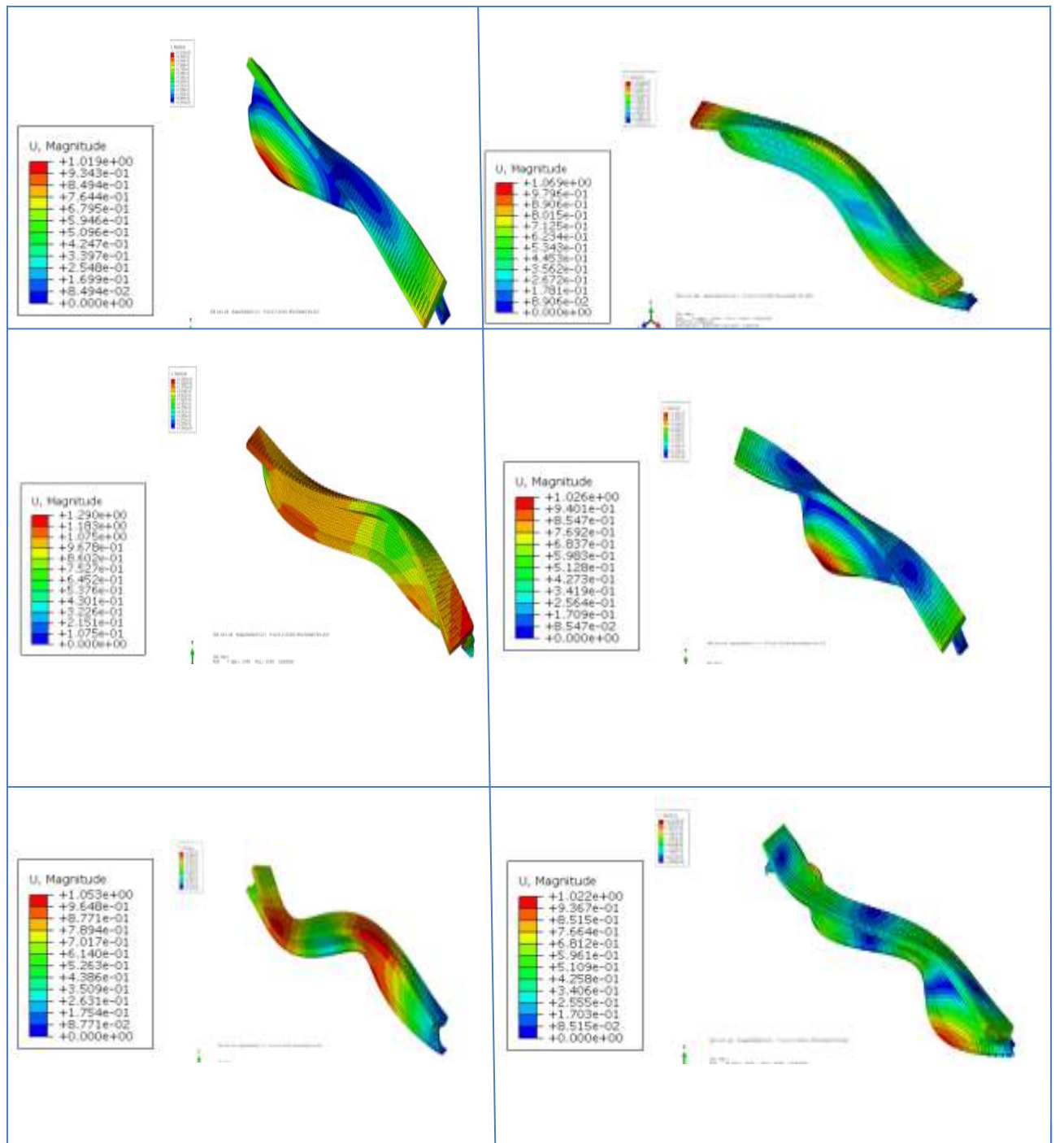


Figure 8-4: The 5th to 10th mode shapes of the model (Case3)

Frame			
Index	Description		
0	Increment	0: Base State	
1	Mode	1: Value = 169.96	Freq = 2.0749 (cycles/time)
2	Mode	2: Value = 780.25	Freq = 4.4457 (cycles/time)
3	Mode	3: Value = 824.69	Freq = 4.5705 (cycles/time)
4	Mode	4: Value = 1270.9	Freq = 5.6739 (cycles/time)
5	Mode	5: Value = 3566.4	Freq = 9.5046 (cycles/time)
6	Mode	6: Value = 3866.9	Freq = 9.8969 (cycles/time)
7	Mode	7: Value = 7002.5	Freq = 13.318 (cycles/time)
8	Mode	8: Value = 7173.4	Freq = 13.480 (cycles/time)
9	Mode	9: Value = 8846.4	Freq = 14.969 (cycles/time)
10	Mode	10: Value = 9276.4	Freq = 15.329 (cycles/time)

Figure 8-5: The first ten natural frequencies of model (Case3)

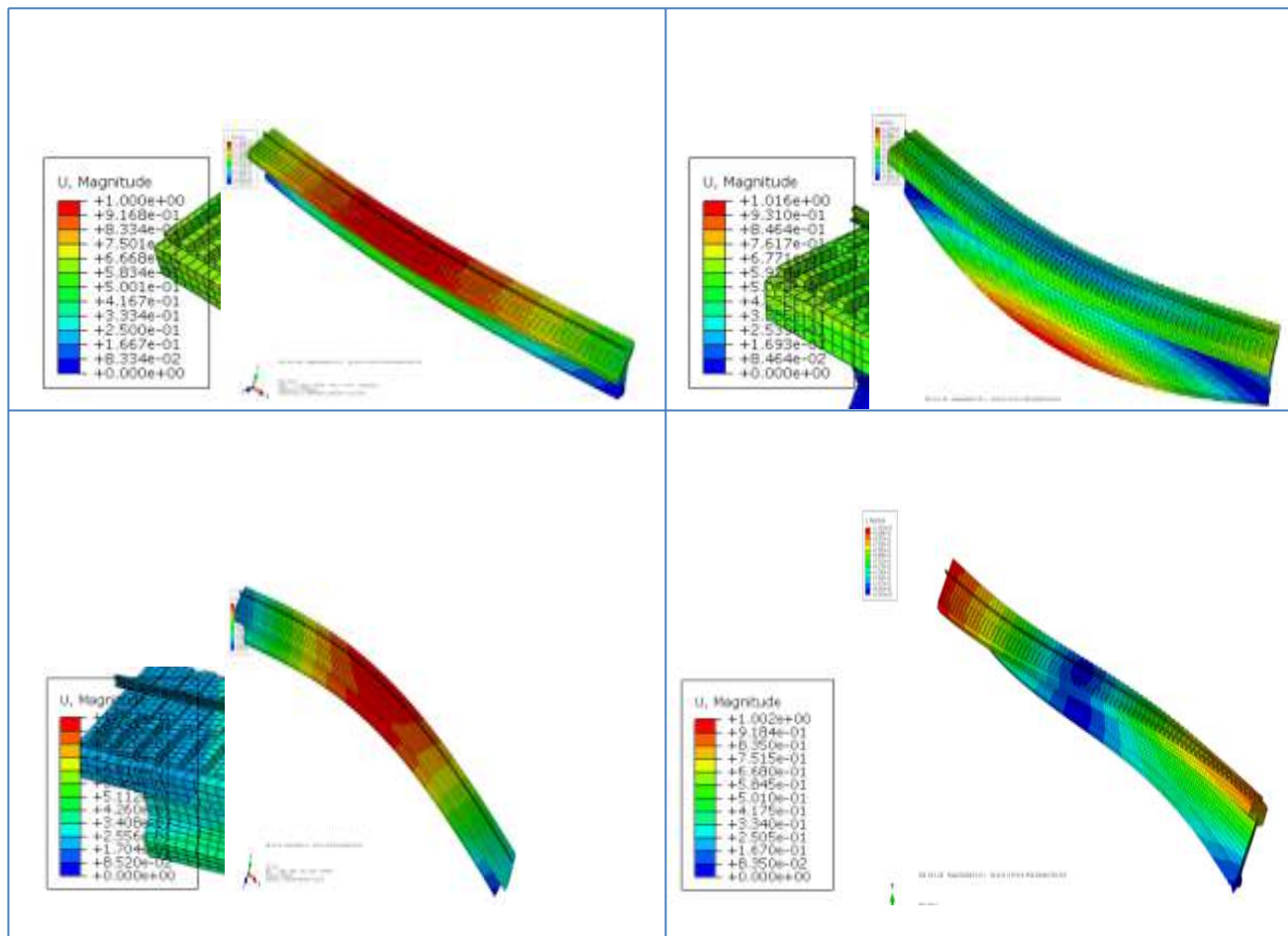


Figure 8-6: The first four mode shapes of the model (Case4)

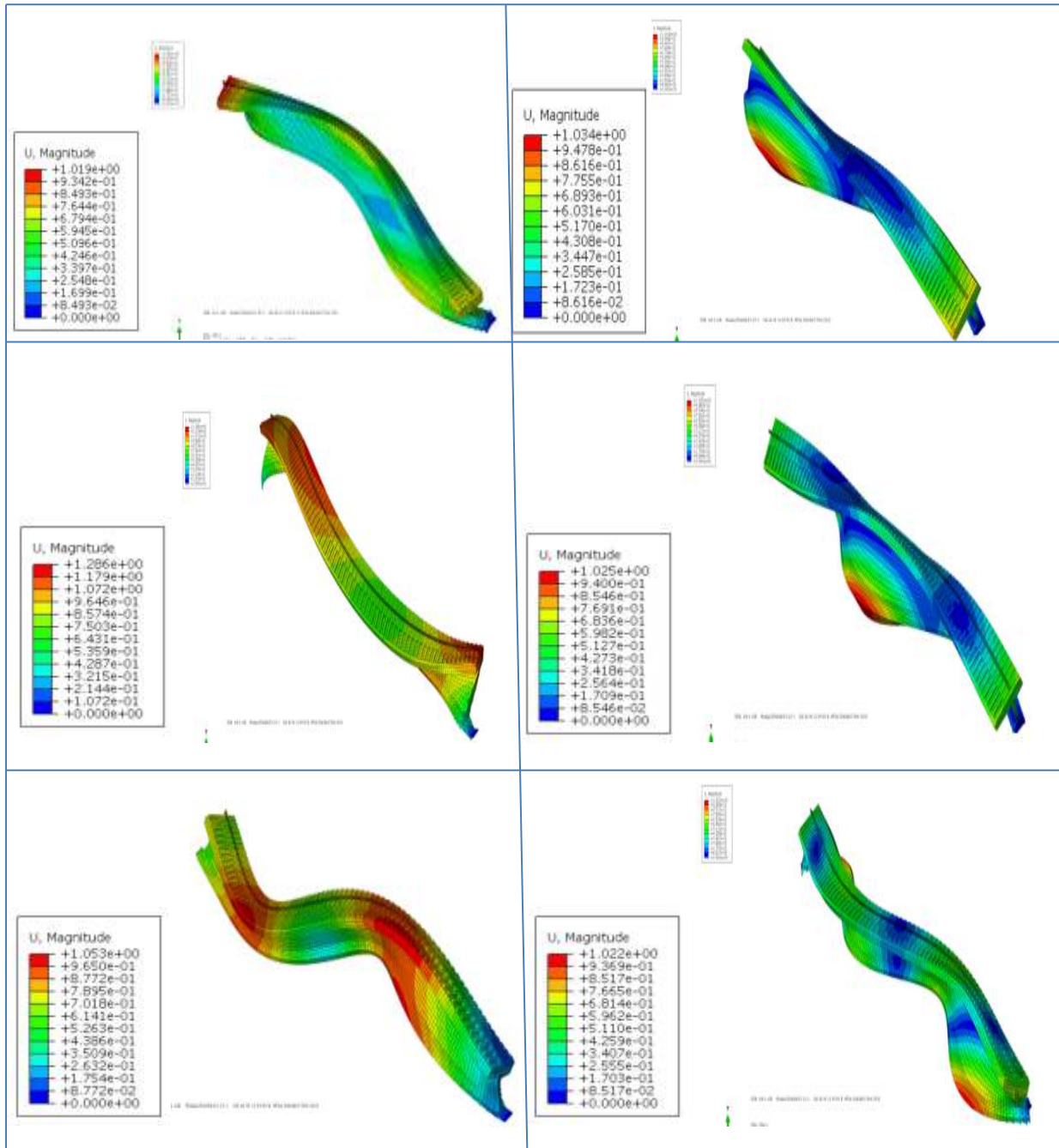


Figure 8-7: The 5th to 10th mode shapes of the model (Case4)

Frame	
Index	Description
0	Increment 0: Base State
1	Mode 1: Value = 170.06 Freq = 2.0755 (cycles/time)
2	Mode 2: Value = 779.05 Freq = 4.4423 (cycles/time)
3	Mode 3: Value = 832.37 Freq = 4.5918 (cycles/time)
4	Mode 4: Value = 1267.3 Freq = 5.6659 (cycles/time)
5	Mode 5: Value = 3570.3 Freq = 9.5098 (cycles/time)
6	Mode 6: Value = 3867.1 Freq = 9.8973 (cycles/time)
7	Mode 7: Value = 7002.8 Freq = 13.319 (cycles/time)
8	Mode 8: Value = 7210.5 Freq = 13.515 (cycles/time)
9	Mode 9: Value = 8849.7 Freq = 14.972 (cycles/time)
10	Mode 10: Value = 9276.1 Freq = 15.329 (cycles/time)

Figure 8-8: The first natural frequencies of the model (Case4)